Granular Matter

Un-jamming due to energetic instability: statics to dynamics

--Manuscript Draft--

Manuscript Number:	
Full Title:	Un-jamming due to energetic instability: statics to dynamics
Article Type:	S.I. : In Memoriam of Robert P. Behringer
Keywords:	constitutive model; un-jamming; jamming; dynamics; concave elastic energy; theory; granular solid hydrodynamics
Corresponding Author:	Stefan Luding Twente University Enschede, NETHERLANDS
Corresponding Author Secondary Information:	
Corresponding Author's Institution:	Twente University
Corresponding Author's Secondary Institution:	
First Author:	Stefan Luding, Prof.
First Author Secondary Information:	
Order of Authors:	Stefan Luding, Prof.
	Yimin Jiang, Prof.
	Mario Liu, Prof.
Order of Authors Secondary Information:	
Funding Information:	
Abstract:	Jamming/un-jamming, the transition be-tween solid- and fluid-like behavior in granular matter,is a ubiquitous phenomenon in need of a sound un-derstanding. As argued here, in addition to the usualun-jamming by vanishing pressure and decrease of den-sity, there is alsoyield(plastic rearrangements and un-jamming that occur) if, for given pressure, the shearstress becomes too large or the density too small. Simi-lar to thevan der Waals transitionbetween vapor andwater, or the critical current in superconductors, we be-lieve that one mechanism causing yield is by the loss ofthe energy's convexity.We focus on this mechanism in the context of a sim-plified version ofgranular solid hydrodynamics (GSH). Even though any other energy-based theory would dis-play similar transitions, only if it would cover granu-lar gas, fluid, and solid states simultaneously could itfollow the systems evolution into un-jammed, possiblydynamic/collisional states – and back to elastically sta-ble ones. We show how the un-jamming dynamics startsoff and unfolds, and propose an approximation schemeto further simplify its account. It is then employed forillustration, to qualitatively follow the system throughvarious deformation modes: transitions, yielding, un-jamming and jamming, both analytically and numerically.
Suggested Reviewers:	Itai Einav itai.einav@sydney.edu.au
	Brian Tighe b.p.tighe@tudelft.nl
	Ken Kamrin kkamrin@mit.edu

Noname manuscript No.
(will be inserted by the editor)

Un-jamming due to energetic instability: statics to dynamics

Stefan Luding · Yimin Jiang · Mario Liu

Received: date / Accepted: date

Abstract Jamming/un-jamming, the transition between solid- and fluid-like behavior in granular matter, is a ubiquitous phenomenon in need of a sound understanding. As argued here, in addition to the usual un-jamming by vanishing pressure and decrease of density, there is also *yield* (plastic rearrangements and un-jamming that occur) if, for given pressure, the shear stress becomes too large or the density too small. Similar to the *van der Waals transition* between vapor and water, or the critical current in superconductors, we believe that one mechanism causing yield is by the loss of the energy's convexity.

We focus on this mechanism in the context of a simplified version of *granular solid hydrodynamics* (GSH). Even though any other energy-based theory would display similar transitions, only if it would cover granular gas, fluid, and solid states simultaneously could it follow the systems evolution into un-jammed, possibly dynamic/collisional states – and back to elastically stable ones. We show how the un-jamming dynamics starts off and unfolds, and propose an approximation scheme to further simplify its account. It is then employed for illustration, to qualitatively follow the system through various deformation modes: transitions, yielding, un-jamming and jamming, both analytically and numerically.

Keywords constitutive model · un-jamming · jamming · concave elastic energy · GSH

Stefan Luding
University of Twente, The Netherlands

Yimin Jiang
Central South University, Changsha, China

Mario Liu
University Tübingen, Germany

Dedication: SL *Bob was not only an inspiring researcher and colleague for me, he influenced my research on granular matter so much! Also he became a good friend over the 25 years I knew him. I will always remember the great research visits to Duke, but also the time we spent together on many international conferences, like in Cargese or at several Powders & Grains events. His passing away was a shock and leaves a big gap for me.*

Dedication: ML *It was in the heydays of helium physics when I, playing with some theories, first met Bob, the conscientious and meticulous experimenter, whose results are wise not to doubt, around which you simply wrap your model. But grains were his real calling. Many decades later, I am again busy fitting my pet theory to his data, and that of his group – such as shear jamming. Some things just never change.*

1 Introduction

The macroscopic Navier-Stokes equations allow one to describe Newtonian fluids with constant transport coefficients (e.g., viscosity). In many non-Newtonian systems, especially granular matter, the transport coefficients depend on various state variables such as the density and the granular temperature. This interdependence and the presence of energy dissipation is at the origin of many interesting phenomena: clustering, shear-band formation, jamming/un-jamming, shear-thickening or shear-jamming, plastic deformations, related also to creep/relaxation, and many others; see the chronologically sorted references (which are cited below, where relevant): [1,2,3,4,5,6,7,8,9,10,11,12, 13,14,15,16,17,18,19,20,21,22,23,24,25,26,27,28,29, 30,31,32,33,34,35,36,37,38,39,40,41,42,43,44,45,46, 47, 48, 49, 50, 51, 52, 53, 54, 55, 56, 57, 58, 59, 60, 61, 62, 63, 64, 65], of which a good fraction was inspired by Bob Behringer.

Some open questions are: *How can we understand those phenomena that originate from the particle- or meso-scale, which is intermediate between atoms and the macroscopic, hydrodynamic scale? And how can we formulate a theoretical framework that takes the place of the Navier-Stokes equations?*

A universal theory must involve all states granular matter can take, i.e., granular gases, fluids, and solids, as well as the transitions between those states. *What are the state variables needed for such a theory? And what are the parameters (that we call transport coefficients) and how do they depend on the state variables?*

Main goal of this paper is to propose a minimalist candidate for such an universal theory, able to capture granular solid, fluid, and gas, as well as various modes of transitions between these states. The model, remarkably, involves only four state variables, density, momentum density (vector), elastic strain (tensor), and granular temperature. It is a boiled down, simplified case of the more complete theory GSH [66, 67, 68, 69, 70, 71]. For the sake of transparency and treatability, we also reduce most transport coefficients and parameters to constants – without loss of generality.

Each transport coefficient is related to the propagation or evolution of one (or more) of these quantities that encompass the present state of the system. For simple fluids [3, 72], it is possible to bridge between the (macroscopic) hydrodynamic and the (microscopic) atomistic scales; as an example, the diffusion coefficient quantifies mass-transport mediated by microscopic fluctuations.

In the case of low density gases, the macroscopic equations and the transport coefficients can be obtained using the Boltzmann kinetic equation as a starting point. For moderate densities, the Enskog equation provides a good, quite accurate description of dense gases (or fluids) of hard atoms [3] or of particles including the effects of dissipation [10], reaching out (empirically) towards realistic systems [73], and beyond, see, e.g., [48, 60]. At the limit of granular fluids, other coefficients, like the viscosity, actually are observed to diverge [48, 74, 75] when the granular fluid becomes denser and approaches jamming to the state that we could call a granular solid, as related to the classical solid mechanics [76]. One objective of this paper is to bring together fundamental theoretical concepts of continuum mechanics [77, 78, 71, 79, 55] with observations made from particle simulations for simple granular systems in the gas, fluid, and solid states, including also the transitions between those states [73, 80, 81, 82, 75, 53].

1.1 About states of granular matter

When exposed to external stresses, grains are elastically deformed at their contacts. In static situations, there is only elastic energy; in flowing states, some of the elastic energy is transferred to the kinetic one and back.[1]

The capability of granular solids to remain quiescent, in mechanical equilibrium, under a given finite stress is precarious. If pressure or shear stress become too large, the grains will, suddenly, start moving – with a vanishing elastic stress. This qualitative change in behavior is an unambiguous phase transition. We shall refer to the region capable of maintaining the equilibrium of static grains as *elastic*, and its boundary (in the space spanned by the state variables) as the *yield surface*.

Granular systems will also un-jam for vanishing pressure and a continuous reduction of density, though we reserve the term yield for the (sudden) loss of elastic stability: Grains un-jam in either case, they *yield* only when the elastic stress, in particular the pressure, is finite.

Starting from the elastic region, decompression (tension) reduces the density and the elastic deformations of the grains – until the latter vanish and the system unjams. Decompressing further just reduces the density accordingly. The system is now un-jammed in the sense that one can change the density without any restoring force, i.e., the elastic energy remains zero. In reverse, compression only increases the density, as long as it is smaller than the jamming density. At jamming both the elastic deformations and the associated energy start to increase with density.

In contrast, there is a discontinuity leaving the elastic regime at finite values of elastic stress. It is a sudden transition from quiescent, enduringly deformed grains to moving ones oscillatorily deformed. This transition needs to be explained, to have a model for. And it is clear that the transition must be encoded in the elastic

[1] Flowing states, as defined here, range from dilute granular gases via inertial, collisional granular fluids, to quasi-static flows, granular solids, e.g., perturbed by elastic waves, excluding only static, elastic solids. Granular solids and quasi-static flows show both solid and fluid features [52], in particular a considerable permanent elastic energy. The ratio of kinetic to potential, elastic energy in the system, $K = E_{\rm kin}/E_{\rm pot}$, is one way to characterize its state: gas ($K \gg 1$), dense collisional flow ($K \sim 1$), quasi-static flow ($K \ll 1$), granular solid ($K \approx 0$), static ($K = 0$) and the extreme, athermal case ($K \equiv 0$, maintained at all times), as can be realized by energy minimization, e.g., see Ref. [82] and references therein. The contribution of potential energy to the total energy is thus $1/(1 + K)$, and the fraction of the total energy that is exchanged between the kinetic and potential energy is then: gas ($w_T/w = 2/(1+K) \ll 1$), collisional ($w_T/w \sim 1$), quasistatic and solid ($w_T/w = 2K/(1 + K) \approx 2K \ll 1$).

energy – the only quantity characterizing the quiescent state – not in the (inactive) dynamics.

In the elastic region, grains appear solid when at rest, but they will flow if subject to an imposed shear rate, and appear liquid. This *continuous change in appearance* is well accounted for by any competent dynamic theory or rheology, it is not a transition [2]. Moreover, flowing grains in the elastic region do sport a macroscopic elastic shear stress, with an associated elastic energy (even though granular contacts switch continually), something no Newtonian liquid is capable of. Also, the shear stress remains finite when the grains stop flowing, which is not the case in Newtonian fluids.

So there are two different flowing states, either with finite elastic stress/strain, or with vanishing ones, which includes granular gases as accounted for by the kinetic theory, see Ref. [73] and references therein. There is also a transition between them. We take both transitions, either leaving the quiescent state, or the flowing one, as the same transition, with the same underlying physics. (In fact, encoding the first transition in the elastic energy certainly affects the flowing state as well.)

We also assume that the elastic energy possesses only a single mechanism for yield, irrespective whether the pressure or the shear stress is too large, or the density too small, as traditionally encompassed by concepts like plastic potentials, yield functions, or flow rules [40, 77,78], see Fig. 1 below and textbooks like Ref. [77].

1.2 Relation to other systems in physics

We do not think that the transition is due to *spontaneously broken translational symmetry* – the usual mechanism giving rise to static shear stresses, as in any fluid-solid transitions. The quick argument is: Consisting of solid, grains already break translational symmetry. More importantly, the loss of equilibrium and granular static is caused by the shear stress or pressure being too strong. This is an indication of an over-tightening phenomenon, of which the (pair-breaking) *critical current* is a prime example.

If a superconductor conducts electricity without dissipation, it is in a *current-carrying equilibrium state*. If, however, the imposed current exceeds a maximal value, the system leaves equilibrium and enters a dissipative, resistive state. The superfluid velocity, $v_s \sim \nabla\phi$, given by the gradient of a quantum mechanical phase, is the analogue of the strain. The dissipationless current, $j_s = \partial w/\partial v_s$, given by the derivative of the energy with respect to v_s, is the analogue of the elastic stress. The over-tightening transition in superconductivity is well accounted for by an inflection point, at which the energy turns from stably convex to concave, see the classic paper by Bardeen [86]. The close analogy between the two systems is a good reason to employ the same approach here, to postulate that the surface of the cone in Fig 1 is an inflection surface of the elastic energy.

1.3 About elastic granular matter

The granular solid state is contingent on granular matter capable of being elastic, for which there is ample evidence, see e.g. Refs. [87,6,88,11,89,90,30,81,49] and references therein. In addition to the material stiffness, many other material properties (including cohesion, friction, surface-roughness, particle-shape) determine the elastic response of granular matter. For soft and stiff materials the deformations are, respectively, considerable and slight, but never zero. Because of their Hertz-like non-linear contacts, grains are infinitely soft in the limit of vanishing contact area (deformation). Therefore, at any given finite force, deformations are always sufficiently large to display the full spectrum of elastic behavior, including a considerable static shear stress (enabling a tilted surface), and elastic waves. Even the simplest model material, consisting of perfectly smooth spheres of isotropic, linearly elastic material, displays non-linearity due to their Hertz-type contacts, on-top of the contact network (fabric) and its re-structuring. Only in computer simulations is it possible to remove the first and focus on the second, see e.g. Ref. [53].

Elastic waves propagate in granular media, displaying various non-linear features, including anisotropy and dispersion, see e.g. Ref. [91,92,93] and references therein. The discreteness and disorder of granular media add various phenomena – already for tiny amplitudes – such as dispersion, low-pass filtering and attenuation [94,93,95]. With increasing amplitudes, a wide spectrum of further phenomena is unleashed, among which the beginning of irreversibility and plasticity, see Ref. [59] in this topical issue, and references therein, and the loss of mechanical stability [96], what we call "yield" in the following.

[2] This is the macroscopic view on a representative volume much larger than the single particles; whether plastic granular flow and elastic instability transitions are connected on a local scale of a few grains is not excluded here, since there is ample evidence of local instabilities, force-chain buckling, trimer deformations, etc., see Refs. [4,83,35,84,58,85], on the particle scale, which is not addressed in this paper.

1.4 Yield: About the limits of elasticity

To envision the *yield surface*, we consider the space spanned by three parameters: pressure P, shear stress σ_s, and void ratio $e = (1-\phi)/\phi$ (where $\rho = \rho_p \phi$, with material density ρ_p and volume fraction ϕ), ignoring the granular temperature (i.e., fluctuations of kinetic energy), as discussed in Ref. [97] and so many papers following. Based on the observation of the *Coulomb yield* and the *virgin consolidation line*, we assume that the yield surface is as rendered in Fig. 1. Elastic, jammed states, maintained by deformed grains, are stable and static only inside it [3].

The Coulomb yield line, see Fig. 1(b), can be reached by increasing the shear stress at given confining pressure. When the shear stress exceeds a certain level, the system yields, un-jams and becomes dynamic. No static, stable elastic state exists above the Coulomb yield line, as evidenced by a sand pile's steepest slope.

It is imperative to realize that (what we call) the Coulomb yield line is conceptually different from the peak shear stress achieved during the approach to the critical state at much larger strains. Coulomb yield is the collapse of static states – such as when one slowly tilts a plate carrying grains until they start to flow (max. angle of stability). Its behavior is necessarily encoded in the system's energy, because this phenomenon does not at all involve the system's dynamics. The critical state, including the peak shear stress – though referred to as "quasi-static" – is a fully dynamic and irreversible effect. It is accounted for by *the stationary solution at given strain rates* in GSH. The angle of repose (always smaller than the max. angle of stability) is in GSH given by the critical friction angle [70, 71].

In the absence of shear stresses, the maximally sustainable pressure depends on the void ratio, e, as rendered in Fig. 1-(a). Starting from a given e, slowly increasing P, the grain-structure will collapse and yield at this pressure, to a smaller value of e, such that the final state is stable, static, and below the curve of Fig. 1-(a). This is because when applying a slowly increasing pressure, the point of collapse is (ever so) slightly above the curve; and the end point below it is typically also close. This evolution resembles a stair-case, with the granular medium increasing its density by hugging this curve, which frequently referred to as the *virgin/primary consolidation line*, or simply the *pressure yield line*. The line cuts the e-axis at the random loosest void ratio, e_0, above which no elastic stable states exists.

[3] However, this does not exclude the possibility that there are plastic deformations possible inside (in finite systems) as evidenced from particle simulations, e.g., in Refs. [22, 81].

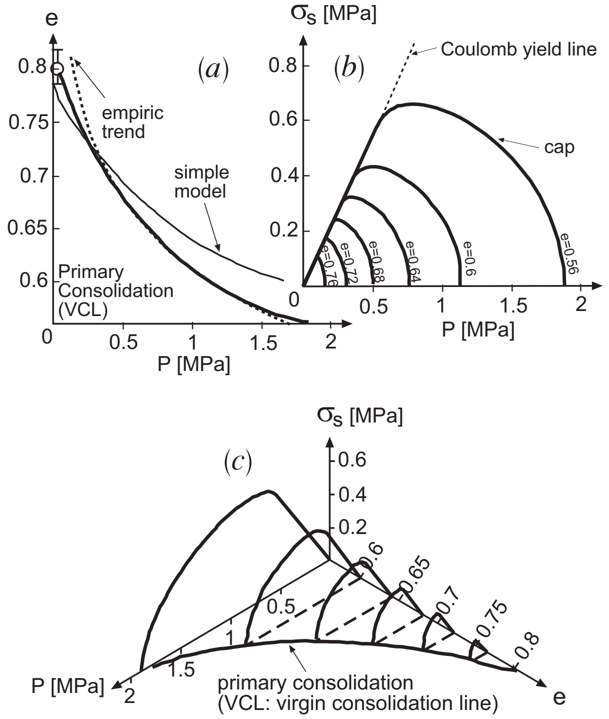

Fig. 1 Granular yield surface, or the jamming phase diagram, for $T_g = 0$, as a function of the pressure P, shear stress σ_s, and void ratio e, as rendered by an energy expression in [69]. Panel **(c)** is the 3D combination of **(a)** and **(b)**; with **(b)** depicting how the straight Coulomb yield line bends over, depending on the void ratio e – a behavior usually accounted for by *cap models* in elasto-plastic theories; while **(a)** depicts the maximal void ratio e (equivalent to the density) plotted against pressure P, or the so-called *virgin consolidation line* (VCL). In panel **(a)**, the dotted line is an empirical relation, $e = e_1 - e_2 \ln(P/P_0)$, with $P_0 = 0.5\,\mathrm{MPa}$, $e_1 = 0.679$ and $e_2 = 0.097$, approximating the VCL, but not valid for $P \to 0$. The thick solid line cuts the e-axis at e_0, with the intersection being the lowest possible, random loosest packing value, see Ref. [69] for details, where also the thin solid line is discussed. Thus e_0 also defines the lowest possible jamming volume fraction, $\phi_{J0} = 1/(1+e_0)$, see Ref. [53], with static, elastic states possible only below the VCL, as will be shown in Secs. 5 and 6.

Because of the pressure yield line, the Coulomb yield curve cannot persist for arbitrarily large P at given e. Rather, it bends over to form a "cap", as rendered in Fig. 1-(b), since an additional shear stress close to the pressure yield line will also cause the packing to collapse. (The shape of the cap depends on the interplay of isotropic and deviatoric deformations as well as the probability for irreversible, possibly large-scale re-structuring events of the micro-structure, or contact network.)

Merging 1(a) and 1(b) yields the elastic region below the yield surface, as given in Fig. 1-(c). Although the e-axis, for $P, \sigma_s = 0$, see Fig.1, is also referred to as the loci of (isotropic) un-jamming, the elastic stress goes continuously to zero here, because the grains are successively less deformed. There is, as already discussed above, no phase transition or yield here.

Next, we summarize all different symbols and nomenclatures, as reference.

1.5 Notation and symbols

This paper is a cooperation of co-authors, whose notational baggage from past publications clash with one another. In the dire need to compromise, we ask the readers to suffer – with us – using varying symbols and notations. Our state-variables are: density, ρ, momentum density, ρv_i, granular temperature, T_g, and the elastic strain, as summarized here.

1. The bulk density, ρ, is related to the volume fraction, $\phi = \rho/\rho_p$ (with ρ_p the particles' material density), the porosity $1-\phi$, and the void ratio $e = (1-\phi)/\phi$. (Later, we shall choose units such that $\rho_p = 1$, so that volume fraction and bulk density are identical.)
2. The conserved momentum density g_i defines the velocity $v_i = g_i/\rho$. The symmetric part of the velocity gradient is

   $$v_{ij} := v_{(i,j)} := \tfrac{1}{2}(\nabla_i v_j + \nabla_j v_i) = -\dot{\varepsilon}_{ij} = D_{ij}$$

   The total strain rate $\dot{\varepsilon}_{ij}$ is positive for compression and negative for tension.
   The symbol v_{ij} is usual in condensed matter physics, see [72,76,98]. It is also the one employed in most previous GSH-publications. The notation D_{ij} is common in theoretical mechanics [78,55], while $\dot{\varepsilon}_{ij}$, or $\dot{\gamma}$, are used, e.g., in soil mechanics and related literature [77].
3. Subscripts, such as i,j,k,l, refer to components of tensors in the usual index notation, with double-indices implying summation, the comma indicating a partial derivative, as in $v_{(i,j)}$; the superscript * denotes the respective traceless (deviatoric) tensor. Using the summation convention, the volumetric strain-rate is abbreviated as: $\dot{\varepsilon}_v = \dot{\varepsilon}_{ll} = -v_{ll} = -D_{ll} = -\mathrm{tr}\mathbf{D}$, where the last term is in symbolic tensor notation. The deviatoric strain-rate is thus $\dot{\varepsilon}^*_{ij} = -v^*_{ij} = -D^*_{ij}$, with the norm $v_s := \sqrt{v^*_{ij}v^*_{ij}} = \dot{\gamma} = D_s = (2J_2^D)^{1/2}$, where J_2^D is the second deviatoric invariant, insensitive to the sign convention.
4. The elastic strain, $\varepsilon^e_{ij} \equiv -u_{ij}$, is the tensorial state variable on which the elastic (potential) energy depends [4]. It is always well-defined and unique, in contrast to the total or plastic strains, which are not, and thus will not be used as state variables for (constitutive) modeling. The respective strain rates, however, are well-defined and thus are used. The strain rate was already given (see item 2.), $\dot{\varepsilon}_{ij} = -v_{ij}$, so that the plastic strain-rate is *defined* as: $\dot{\varepsilon}^p_{ij} = \dot{\varepsilon}_{ij} - \frac{d}{dt}\varepsilon^e_{ij}$ (see also item 7.).
5. The isotropic elastic strain

   $$\Delta := -u_{ll} = \varepsilon^e_{ll} = \varepsilon^e_v = \ln(\rho/\rho_J)$$

   is positive for compression. It may be seen as the true strain relative to a stress-free reference configuration – if $\Delta > 0$. Arriving at $\Delta = 0$, the system un-jams and the jamming density $\rho_J = \rho$ is the actual one ρ. [5]
6. The norm of the deviatoric elastic strain is, in accordance to the general scheme, $u_s = \sqrt{u^*_{ij}u^*_{ij}} = (2J_2^u)^{1/2}$.
7. In general, we take $\frac{\partial}{\partial t}$ as the partial time derivative, and $\frac{d}{dt}$ as the total one, including all convective terms. Hence, with the vorticity tensor given as $\Omega_{ij} \equiv v_{[i,j]} \equiv \frac{1}{2}(\nabla_i v_j - \nabla_j v_i)$, one has (as example) the total time derivative of the elastic strain

   $$\tfrac{d}{dt}\varepsilon^e_{ij} = \left(\tfrac{\partial}{\partial t} + v_k\nabla_k\right)\varepsilon^e_{ij} + \Omega_{ik}\varepsilon^e_{kj} - \varepsilon^e_{ik}\Omega_{kj}\ . \qquad (1)$$

   Being off the focus here, the convective terms are usually neglected, so that $\frac{d}{dt} \equiv \frac{\partial}{\partial t}$. The dots in $\dot{\varepsilon}^p_{ij}$ and $\dot{\varepsilon}_{ij}$ are only a (convention preserving) indication of rates, but do not represent the mathematical operation above.
8. The total stress is not an independent state variable, but rather given by the energy density and entropy production, as discussed in the classical GSH

[4] Note the different signs in the last two terms, i.e., the isotropic elastic strain, $\Delta = \varepsilon^e_v$, is positive for compression, whereas u^*_{ij} is negative (if eigenvalues are considered).

[5] Generalizing GSH, we allow negative elastic strains $\Delta = \varepsilon^e_v$ here, interpreting it as the separation distance between particles – or their mean free path – in order to catch both jammed and un-jammed situations. Note that the elastic energy of a negative Δ is identically zero, and that a negative Δ is not independent of the density ρ. Compressing from an un-jammed state, the system jams at $\Delta = 0$, towards $\Delta > 0$ and $\rho > \rho_J$. In isochoric situations (constant density), an evolution of the state variable, Δ, the isotropic elastic strain, implies an evolution of the (enslaved, dependent) jamming density, $\rho_J = \rho\exp(-\Delta)$, as proposed and studied in detail in Ref. [53]. The physics clearly changes between positive (jammed) and negative (un-jammed) states, but for the sake of brevity, below jamming, we limit $\rho_J \geq \rho_{J0}$ and thus $\Delta(\rho) = \ln(\rho/\rho_{J0})$, in cases where it would drop below its absolute limit, ρ_{J0}, which can be seen as the random loosest packing density.

literature. In the simplified version, it may be written as $\sigma_{ij} = \pi_{ij} + P_T\delta_{ij} + \sigma_{ij}^{\text{visc.}}$, with elastic, kinetic/granular temperature and viscous contributions. The isotropic stress is referred to as pressure, $P = \frac{1}{3}\sigma_{kk}$, and the elastic pressure is $P_\Delta = \frac{1}{3}\pi_{kk}$, for three dimensions $\mathcal{D} = 3$.

9. The symbols B and G are used in the definition of the isotropic and deviatoric (shear) elastic energy density. In previous GSH-papers [69, 70, 71], the symbol A was used for G, the classical symbol, but since A is referred to as the anisotropy modulus in other studies, see Ref. [53], we stick to G here [6].
10. The granular temperature used in GSH is T_g, that in kinetic theory and DEM is denoted as T_G or T_K. Comparing GSH-formulas in the gas limit to that of the kinetic theory [1, 10, 73, 34], one should remember

$$T_g^2 \sim T_G \ , \tag{2}$$

but we will only use T_g here. (In this paper, T_g has the units of velocity scaled by the particle diameter, i.e., that of an inverse time, or a rate.) [7].

1.6 Overview

In what follows, we shall, in Sec. 2, consider the significance of an inflection surface, of a convex-concave transition in the energy, as relevant for classical systems, transiently elastic systems and granular matter. We then present review of and a minimalist version of GSH in Sec. 3, allowing for analytic solutions in Sec. 4, and numeric calculations in Sec. 5, before we conclude in Sec. 6.

[6] Note that (calligraphic) symbols $\mathcal{B} \neq B$, $\mathcal{G} \neq G$, and $\mathcal{A}$, in general, are the (tangent) moduli, representing the second derivatives of the elastic energy density with respect to isotropic and deviatoric strain, or mixed, respectively; symbols $\mathcal{B}_\Delta$, $\mathcal{G}_\Delta$ are again different and are the secant moduli; for more details see subsection 3.2.1.

[7] The two temperatures T_g and T_G are different in the following sense. In thermal equilibrium of a static granular solid, T_g becomes equal to the true temperature, $T_g = T$. In granular gases, if thermal equilibrium could ever be reached, we have $T_G = T$ – a relevant condition if one starts to consider the dissipation and heating of the grains. By ignoring T_G's role as a "temperature" of the granular degrees of freedom, taking it only as a measure of the velocity fluctuation squared, $T_G \sim |\delta v_i|^2$, one may go on using T_G in denser ensembles. Conversely, one may use T_g in granular gases, taking it as $T_g \sim |\delta v_i|$. However, while $T_g = T$ does hold in granular static equilibrium, $T_G = T$ can never be reached, as any finite T_G, for finite sized particles, translated into temperature, leads to values of order of the inner temperature of the sun. Only in the atomic/molecular limit of "particles" one has T_G analogous to $k_B T$. It is therefore more sensible to employ T_g throughout.

2 Equilibrium conditions and dissipative terms

In this section, we first revisit the reason for thermodynamic energy's convexity, and derive the equilibrium conditions for three systems: elastic, transiently elastic and granular media. There is one equilibrium condition for each state variable, that maximizes its contribution to entropy or, equivalently, minimizes its contribution to energy. Examples for equilibrium conditions are uniform temperatures and uniform stresses. As these conditions represent extremal points, the energy needs to be convex to be minimal, for the system to be stable.

Then we make the general point that every equilibrium condition, if not satisfied, is a dissipative channel that gives rise to a negative/dissipative term in the evolution equation of the associated state variable. As a result, the state variable relaxes, towards satisfying the condition. In a closed system, all variables will eventually satisfy all their respective conditions, which is the state we called equilibrium.

If the energy is concave, equilibrium conditions represent maxima of the energy with respect to variation of a state-variable. The dissipative terms will thus drive the system away from equilibrium, producing, e.g., non-uniformity in temperature and stress fields. When this happens, what micro-mechanical mechanisms it originates from, is necessarily more specific. How the dynamics further evolves depends on the system one considers. In the classical *van der Waals theory* of the gas-liquid transition, droplet formation is the basic mechanism. In granular media, we propose the following mechanism.

In the stable region, within the cone of Fig 1, the dissipative term in the equation for the elastic strain serves to maintain stress uniformity. It remains inconspicuous as long as one studies the evolution of uniform stresses. Outside the yield surface, it forces the system to leave stress uniformity. Non-uniform stresses accelerate grains in varying directions, producing jiggling and thus granular temperature which, in turn, allows the stress to relax, pushing the system back into the convex region.

This is what we believe happens in grains at yield and beyond the transition. Setting up a dynamical model for following the system through the transition to different states is the main purpose of this paper.

2.1 Elasticity

Consider an elastic system characterized by two state variables, the entropy density, s, and the elastic strain,

$$-\varepsilon_{ij}^e \equiv u_{ij} = \tfrac{1}{2}(\nabla_i U_j + \nabla_j U_i), \tag{3}$$

with a thermodynamic energy density that is a function of both, $w = w(s, u_{ij})$ [76].

A textbook proof of energy convexity considers only the entropy as a variable, and involves an elastic system connected to a heat bath. A temperature fluctuation (associated to entropy fluctuations) vanishes only if the energy is larger with it than without, which is shown to imply convexity [99]

In a more general consideration, we start with the assumption that the system is stable and has an equilibrium for given values of s and u_{ij}. Since the elastic stress, $\pi_{ij} \equiv -\partial w/\partial u_{ij}$ is symmetric, $\pi_{ij} = \pi_{ji}$, we may write the total differential of the energy density as:

$$\mathrm{d}w = T\mathrm{d}s - \pi_{ij}\mathrm{d}u_{ij} = T\mathrm{d}s - \pi_{ij}\mathrm{d}\nabla_j U_i\,, \tag{4}$$

with temperature $T = \partial w/\partial s$. We varied this energy by (i) keeping $\int s\mathrm{d}V = const.$, or $\delta \int (w - T_L s)\, \mathrm{d}V = 0$ with $T_L = const.$ a Lagrange parameter; (ii) forbidding external work $\oint \pi_{ij}\delta U_i\, \mathrm{d}A_j = 0$; and (iii) using Gauss' theorem [8], the result is

$$\begin{aligned} 0 &= \int [T\delta s - \pi_{ij}\delta\nabla_j U_i - T_L\delta s]\ \mathrm{d}V \\ &= \int [(T - T_L)\,\delta s + (\nabla_j \pi_{ij})\,\delta U_i]\ \mathrm{d}V. \end{aligned} \tag{5}$$

With δs and δU_i varying independently, and $T_L = const.$, the equilibrium conditions may be written as

$$\nabla_i T = 0, \quad \nabla_j \pi_{ij} = 0. \tag{6}$$

These are extremal conditions. They represent an energy minimum and stable equilibrium, only if deviations from them yield an energy increase. Therefore, inserting $T = T^{eq} + \delta T$, $\pi_{ij} = \pi_{ij}^{eq} + \delta\pi_{ij}$, with $\nabla_i T^{eq} = 0$ and $\nabla_j \pi_{ij}^{eq} = 0$, we require

$$\delta^2 w = \delta T \delta s - \delta\pi_{ij}\delta u_{ij} > 0. \tag{7}$$

Assuming first $\delta u_{ij} \equiv 0$, we may write $\delta^2 w = \delta T \delta s = (\partial T/\partial s)(\delta s)^2 > 0$, implying

$$\frac{\partial^2 w}{\partial s^2} = \frac{\partial T}{\partial s} > 0,$$

or that the energy w is a convex function of s. As a result, temperature fluctuations will diminish, and the state characterized by a uniform temperature is a stable equilibrium. Conversely, if the energy is concave, $\partial^2 w/\partial s^2 < 0$, the condition $\nabla_i T = 0$ represents a maximum of energy, and the system is unstable. Any fluctuations in entropy will move it away from uniform temperature. In the case of the van der Waals transition between gas and liquid, a uniform single-phase system is moved to the coexistence of two phases, with different entropy densities, but the same temperature.

Next, as used explicitly below, in subsection 3.2.1, assuming $\delta s \equiv 0$, we order the six components of π_{ij} and u_{ij} each as a 6-tuple vector, denoted by Greek letters, and require

$$\delta^2 w = -\delta\pi_{ij}\delta u_{ij} = -\delta\pi_\alpha \delta u_\alpha = \frac{\partial \pi_\alpha}{\partial u_\beta}\delta u_\alpha \delta u_\beta > 0. \tag{8}$$

This implies that the 6x6 Hessian matrix

$$\frac{\partial^2 w_e}{\partial u_\alpha \partial u_\beta} = -\frac{\partial \pi_\alpha}{\partial u_\beta} \quad \text{has only positive eigenvalues,} \tag{9}$$

implying that the energy w is a convex function of the elastic strain u_{ij}. If there is at least one negative eigenvalue, the condition $\nabla_j \pi_{ij} = 0$ no longer represents a stable state, because along the associated eigenvector, the energy is a maximum. The system can and will escape, initially by violating $\nabla_j \pi_{ij} = 0$, typically rendering the stress non-uniform.

To obtain static elastic solutions, we solve $\nabla_i \pi_{ij} = 0$ for given boundary conditions. This is equivalent to looking for minima of the elastic energy. The solutions are stable if the elastic energy is convex. They are unstable otherwise, and devoid of physical significance.

The more general consideration, including both δs and δu_{ij}, leads to a 7x7 matrix that, for stable equilibria, must possess seven positive eigenvalues.

A complete consideration for elasticity requires also the inclusion of the density, ρ, and momentum density ρv_i as the energy's variables. This, being somewhat more lengthy, would distract from the present concern. The associated equilibrium conditions, with the gravitational acceleration, g_i, and the chemical potential given as $\mu = \partial w/\partial \rho$ (as derived in Refs. [100, 79]) are:

$$\nabla_i \mu = -g_i, \tag{10}$$

$$-\dot{\varepsilon}_{ij} \equiv v_{ij} \equiv \tfrac{1}{2}(\nabla_i v_j + \nabla_j v_i) = 0, \tag{11}$$

$$\nabla_i P = s\nabla_i T + \rho \nabla_i \mu = -\rho g_i\ . \tag{12}$$

The force equilibrium $\nabla_i P = -\rho g_i$ is a direct result of $\nabla_i T = 0$ and $\nabla_i \mu = -g_i$. All three equations express minimal energy, or maximal entropy.

[8] According to Gauss' theorem, the surface integral transforms as: $\oint \pi_{ij}\delta U_i\, \mathrm{d}A_j = \int \nabla_j(\pi_{ij}\delta U_i)\mathrm{d}V = \int [(\nabla_j \pi_{ij})\delta U_i + \pi_{ij}\delta\nabla_j U_i]\, \mathrm{d}V = 0$. Using the definition of the stress or traction vector, $t_i = \pi_{ij}\hat{n}_j$, the surface integral can be rephrased, $\oint \pi_{ij}\delta U_i\, \mathrm{d}A = \oint t_i \delta U_i\, \mathrm{d}A$, allowing to add tractions (or point/contact forces) at the surface of V, which would pop up on the right hand side of Eq. (5) but are not used here.

If any of the equilibrium conditions are not satisfied, dissipative currents appear to counteract: [9] heat diffusion $\sim \nabla_i T$ in the evolution equation for s, viscous stress $\sim v_{ij}$ in the evolution equation for ρv_i, and a term $\sim \nabla_k \pi_{ik}$, in the equation for the displacement,

$$\frac{\partial}{\partial_t} U_i - v_i = -\beta \nabla_k \pi_{ik}. \tag{13}$$

(Analogous to heat-conductivity, β quantifies the strength of the dissipation. Taking it as a scalar is an approximation.) All these terms serve the sole purpose of restoring the respective equilibrium conditions: $\nabla_i T, v_{ij}, \nabla_k \pi_{ik} = 0$.

The dissipative "displacement rate" $\sim \nabla_k \pi_{ik}$, as a necessary result of thermodynamics, has been first recognized in the classical 1972-paper: *"The unified hydrodynamic theory for crystals, liquid crystals, and normal fluids"*, by Martin, Paraodi and Pershan [98]. It drives the system, boundary conditions permitting, toward a constant stress. If the stress is not constant, such as in elastic waves, it contributes to wave damping. If one concentrates on the evolution of constant stresses, this term vanishes and is irrelevant. However, if the energy is concave, this term wracks havoc by driving the system away from uniform stresses. Writing it in the notation of the 6x6 matrix, Eq. (9), as:

$$\nabla_k \pi_{jk} \to \nabla_k \pi_\alpha = \partial \pi_\alpha / \partial u_\beta \nabla_k u_\beta \ , \tag{14}$$

we see that, if the matrix $\partial \pi_\alpha / \partial u_\beta$ has a negative eigenvalue, the corresponding term will its flip sign. Instead of keeping the stress uniform, it drives the stress towards non-uniformity. This in turn accelerates mass points, possibly leading to non-uniform velocities v_i and thus finite strain rates, $v_{ij} \equiv -\dot{\varepsilon}_{ij}$. Initially, the stress perturbation will grow along the direction associated with the negative eigenvalue, but for finite times, this is by no means true, as the system will try to move towards a stable equilibrium state, whatever that is. See the next two sections what happens in granular matter.

Eq. (13), in term of the elastic strain, Eq. (3), reads

$$\begin{aligned} \frac{\partial}{\partial t} u_{ij} - v_{ij} &\equiv -\frac{\partial}{\partial_t} \varepsilon^e_{ij} + \dot{\varepsilon}_{ij} \\ &= -\nabla_i [\beta \nabla_k \pi_{jk}] - (i \leftrightarrow j) \equiv p_{ij} \ , \end{aligned} \tag{15}$$

where the double-arrow indicates the (non-symmetric) counterpart of the preceding term. Eq. (15) seems to suggest that the dissipative term p_{ij} is simply the plastic strain rate, $p_{ij} = \dot{\varepsilon}^p_{ij}$, which apparently exists even in solid if the stress is nonuniform. This would be a confusing nomenclature, as none of the typically plastic phenomena such as connected to concepts of plastic potentials or flow functions (see Refs. [77,78]) are addressed here, in the context of elasticity. The term plastic strain rate is more appropriate for the dissipative contributions discussed in the next two sections, on transient elasticity and granular media.

Note that heat diffusion and viscous stress exist in any system, in which entropy and momentum are state variables: liquids, solids, granular media, irrespective of the microscopic interaction. Same holds for the dissipative term p_{ij}, which exists in any system in which the elastic strain is a variable. This is the reason it also exists in granular media. Generally speaking, every dissipative term strives to satisfy its equilibrium condition by changing the value or distribution of the associated state variable. Equilibrium is achieved if all equilibrium conditions are satisfied, as entropy is then maximal.

[9] Deviations from $\nabla_i \mu = -g_i$ do not lead to a dissipative mass current, because the mass current is necessarily given by the momentum density ρv_i. The underlying reason is Galilean invariance, implying the local conservation of the *booster* [100,79].

2.2 Transient elasticity and plasticity

There are many transiently elastic systems in nature. If quickly deformed, they are elastic and capable of restoring their original shape. But this does not happen if the deformation is kept longer; then the deformation is irreversible, plastic. One example are polymeric melts that consist of entangled elastic strands, which elastically deform, but disentangle if given enough time. This leads to a reduction, and eventually vanishing, of the elastic stress. For such systems, the equilibrium condition is:

$$\pi_{ij} = 0, \qquad \text{or, equivalently} \quad u_{ij} = 0 \ . \tag{16}$$

Consequently, the evolution equation (15) takes the form:

$$\dot{\varepsilon}^p_{ij} = \frac{\partial}{\partial t} u_{ij} - v_{ij} \equiv -\frac{\partial}{\partial_t} \varepsilon^e_{ij} + \dot{\varepsilon}_{ij} = -\lambda_e u_{ij} \ , \tag{17}$$

with the plastic strain rate now a relaxation term, with a positive coefficient λ_e. Employing essentially this equation, including the convective terms of Eq. (1), a wide range of polymer behavior including shear thinning/thickening and the Weissenberg or rod-climbing effect were reproduced [101,102].

It is noteworthy that the plastic strain rate in the form $\dot{\varepsilon}^p_{ij} = -\lambda_e u_{ij}$ is a diagonal Onsager term, hence off-diagonal ones such as

$$\dot{\varepsilon}^p_{ij} = \frac{\partial}{\partial t} u_{ij} - v_{ij} = -\lambda T_g u_{ij} - p_{ijkl} v_{kl} \tag{18}$$

are also permitted. They will turn out to be useful in granular physics.

The close link, even identity, between transient elasticity and strain relaxation on one hand, and plastic behavior of irreversible shape change on the other, is a useful insight. Similarly useful is the understanding of the difference between elasticity and transient elasticity. For the latter to be in equilibrium, the elastic stress has to vanish, while a constant stress suffices for the former. For verbal clarity, we denote

$$\begin{aligned} &\text{elastic equilibrium}: \quad \nabla_i \pi_{ij} = 0, \\ &\text{"plastic equilibrium"}: \quad u_{ij} \equiv -\varepsilon^e_{ij} = 0 \ , \end{aligned} \tag{19}$$

where "plastic equilibrium" is short for "transiently elastic, long-term equilibrium".

There is a further subtlety that we must address here. If the polymer energy depends on both the density and the elastic strain, there are two contributions in the stress: the pressure as given by Eq. (12) and the elastic stress. Then the system may possess an equilibrium pressure even when Eq. (19) holds. However, if the density is not an independent state variable, implying $P \equiv 0$, an equilibrium pressure needs a finite $\Delta \equiv -u_{ll}$ to be sustained, and $u_{ij} = 0$ cannot be the equilibrium condition. Rather, it is given as

$$u^*_{ij} \equiv -\varepsilon^{e*}_{ij} = 0, \quad \text{implying} \quad \dot\varepsilon^p_{ij} = -\lambda_e u^*_{ij} \ , \tag{20}$$

the vanishing of the deviatoric part, while the trace Δ, not independent from the density, simply follows the dynamics of the density. It does not relax.

Note that the relaxation time of Δ and u_s need not be the same. If that of Δ is especially long, it may be neglected for certain phenomena, for which the dynamics is governed by $\dot\varepsilon^p_{ij} = -\lambda_e u^*_{ij}$ alone.

When the system is crossing an inflection surface, the term $-\lambda_e u_{ij}$, in Eq. (17) is not affected, and continues to push the elastic strain toward $u_{ij} = 0$.

2.3 Granular matter

GSH was set up in compliance with thermodynamics and conservation laws. Here, we discuss its structural part, necessary if one is to be consistent with the general principles of physics. In Sec. 3, a reduced complete version of GSH, including only some constitutive choices, is presented, which will be employed later to study the jamming and un-jamming dynamics.

Two basic pieces of physics characterize granular media: (1) They have two entropies: s_g for the granular degrees of freedom and s for the much more numerous microscopic ones. (2) Depending on circumstances, granular media may be elastic or transiently elastic. Both elastic and plastic equilibria of Eqs. (19) are therefore relevant. However, note that the equilibrium (limit) state is not necessarily ever reached, neither under permanent deformation, nor under free relaxation. In the former case, the system is permanently pulled away from the equilibrium (steady state is *not equal to* equilibrium), while in the latter, if T_g relaxes fast enough, the equilibrium cannot be realized by the other state variables either.

Including s_g as an extra state-variable, with $T_g \equiv \partial w/\partial s_g$, the equilibrium condition is $T = T_g$, obtained by maximizing $\int (s + s_g) \mathrm{d}V \approx \int \ s\mathrm{d}V$, where $s_g \ll s$ may be ignored. The equilibrium condition implies that all degrees of freedom, microscopic as well as granular ones, will eventually equilibrate with one another. Furthermore, since for particles of grain size, one typically has $T_g \gg T$ by many orders of magnitude, $\sim 10^{10}$, we may set the equilibrium granular temperature to zero,

$$T_g = T \approx 0 \ . \tag{21}$$

In analogy to the relaxation terms discussed above, the evolution equation for s_g must therefore possess a relaxation term $\sim T_g$, pushing s_g towards $s_g \propto T_g = 0$. This dissipation/relaxation takes place due to collisions, with rate $\sim T_g$, or due to elasticity, with rate $\sim T_e$, or both. In addition, analogous to the viscous heating term in the hydrodynamic theory of Newtonian fluids, which transfers kinetic energy into heat, via $\eta v^*_{ij} v^*_{ij} \equiv \eta v_s^2 \to T \frac{\partial}{\partial t} s$, there is a term that transfers kinetic energy into "granular heat", $\eta_g v_s^2 \to T_g \frac{\partial}{\partial t} s_g$. Therefore, assuming $\nabla_i T_g = 0$, and ignoring gradients, the evolution equation for granular energy reads

$$T_g \tfrac{d}{dt} s_g = -\gamma T_g^2 + \eta_g v_s^2 \ , \tag{22}$$

with coefficient $\gamma = \gamma(T_g)$ dependent on T_g, and the compressional viscosity neglected, like convective and diffusive terms, for the sake of brevity. To be used in the following, after some re-writing [10] the evolution equation for granular temperature reads:

$$b\rho \tfrac{\partial}{\partial t} T_g = -\gamma_1 T^*_g T_g + \eta_1 v_s^2. \tag{23}$$

The effective temperature $T^*_g = T_g + T_e$ is discussed in more detail below in Secs. 3.1 and 4.

For given deviatoric (shear) strain rate, $v_s = |v^*_{ij}| = |-\dot\varepsilon^*_{ij}|$, the steady state solution is given and discussed in section 4.5 with the limit case for $\gamma_0 \ll \gamma_1 T_g$, or $T_e \ll T_g$:

$$T_g = T_g^{(ss)} = v_s \sqrt{\frac{\eta_g}{\gamma}} = v_s \sqrt{\frac{\eta_1}{\gamma_1}},$$

[10] Preempting the discussion in Sec. 3, to write down the final evolution equation for T_g, for reasons detailed in [69,70,71], and partially in Sec. 3, we use:

$$s_g = \rho b T_g, \quad \eta_g = \eta_1 T_g, \quad \gamma = \gamma_0 + \gamma_1 T_g, \quad \text{or, equivalently}$$
$$\gamma = \gamma_1 (T_g + \gamma_0/\gamma_1) \equiv \gamma_1 (T_g + T_e) \equiv \gamma_1 T^*_g,$$

in order to work with parameters that do not depend on T_g anymore.
When inserting ρb into Eq. (22) for energy, the time derivative of this variable is neglected.

a result known to hold in granular gases [11], up to moderate densities [10,73]. In this case, the system is in the rate-independent elasto-plastic regime, where the granular temperature is proportional to the strain rate. For diminishing $T_g \ll T_e$ and $\gamma_0 \gg \gamma_1 T_g$, we have an exponential and much faster decay, $\frac{\partial}{\partial t} T_g \propto -T_g$, however, also here the steady state granular temperature persists and remains relevant, as $T_g^{(e)} \approx (T_g^{(ss)})^2/T_e$, see section 4.5.

Returning to the elastic strain u_{ij}, we note that granular media are elastic for quiescent grains, $T_g = 0$, as slopes of sand-piles demonstrate. If the particles "jiggle", $T_g \neq 0$, the elastic shear strain and stress will diminish, and eventually vanish: Tapping a vessel of grains (with a finite number) long (and strong) enough results in a flattened granular surface, like in transient elasticity. Combining both conditions of Eqs. (19), the evolution equation for the elastic strain contains both types of plastic strain rates, see also Eqs. (15,18),

$$\dot{\varepsilon}^p_{ij} = \frac{\partial}{\partial t} u_{ij} - v_{ij} = -\lambda T_g u_{ij} - p_{ijkl} v_{kl} + p_{ij} \ , \qquad (24)$$

where the first term on the right, pushing u_{ij} towards the plastic minimum $u_{ij} = 0$, operates only for $T_g \neq 0$.

The second term represents strain- or stress-driven plastic deformations – occuring well within the macroscopic, elastically stable regime, involving possibly local events, on the particle scale – and will be split up into an isotropic (volumetric) and a deviatoric (shear) contribution, p_v and p_s, with the respective plastic deformation probabilities, see subsection 4.1. The micromechanical origins of these probabilities, are not addressed here, rather see Refs. [22,53,59,84,103,85] and references therein, where it is shown that (finite) granular systems can remain elastic for tiny strain, then have localized plastic events at larger strain, with probability increasing, before (global) yield takes place with particular probabilities as cast into a meso-scale, stochastic master-equation approach, in Refs. [104,105].

The third term depends in particular on the gradient of the elastic stress, see below and Refs. [69,70]. This plastic strain rate, p_{ij}, pushes u_{ij} towards the elastic equilibrium of uniform stress in the energetically convex region, and away from it in the concave one, since the gradient of stress changes sign at the transition.

2.3.1 Dynamics at constant strain or stress

Equation (24), in addition to the dynamics of T_g, Eq. (22), render granular behavior rather more complex than the superposition of behavior from polymers and elastic media. Imposing either a constant shear rate or a constant elastic stress in a polymer melt, Eq. (17), the steady state result is the same, $v_s = \lambda_e u_s$, in either case. This symmetry does not hold for granular media – not even for the simplest case with $T_e = 0$, and $p = 0$.

This symmetry does not hold in grains. A constant shear rate v_s, with the stationary solution $T_g = v_s \sqrt{\eta_g/\gamma}$ (for $T_e = 0$) inserted into Eq. (24), ignoring the p-terms on the r.h.s., leads to a *rate-independent* evolution equation for u_{ij} that possesses the hypoplastic structure [106]. It accounts well for elasto-plastic motion [107], including the approach to the critical state and shear jamming [108,109,70,71].

On the other hand, holding the stress/elastic strain constant, and inserting the stationary limit of Eq. (24), $v_s = \lambda T_g u_s$, into Eq. (22), yields the relaxation rate: $-\gamma_c = (-\gamma + \eta_g \lambda^2 u_s^2)$, negative if $u_s < u_s^c = \sqrt{\gamma/\eta_g}/\lambda$, we find T_g to relax, pushing the system into a static state. The relaxation rate vanishes (i.e., the relaxation time diverges) as the stress (or elastic strain) approaches the critical value and, with a further increase, the rate flips sign to positive above the critical value, see [70,71], creating an ever increasing strain rate v_s. Accordingly, switching from an imposed shear rate (say during an approach to the critical state) to an imposed sub-critical stress will render the system static due to the relaxation of T_g, whereas a critical or super-critical stress will create T_g and thus accelerate the flow, since $v_s \propto T_g$.

2.3.2 Dynamics in the concave region

Within the cone of Fig. 1, in the energetically convex region, as long as one considers only the evolution of uniform stresses, the elastic dissipative term $p_{ij} = \nabla_i[\beta \nabla_k \pi_{jk}] + (i \leftrightarrow j)$ remains zero. Serving to maintain stress uniformity, it may simply be neglected. Yet this term wrecks havoc if the energy is concave.

Perturbing the system by a (local) stress, $\delta\pi_{ij}$, from a static situation, in the convex, stable region, results in a relaxation of the elastic strain, due to the sign of p_{ij}. In contrast, in the concave region, because of Eq. (14), this relaxation turns into an explosion, and drives the stress towards further, stronger non-uniformity.

This accelerates the grains, locally, leading to nonuniform velocities v_i and finite strain rates, $v_{ij} \equiv -\dot{\varepsilon}_{ij} \neq 0$. The latter serve as a source for granular heat, see Eq. (22), and create considerable T_g, which activates the first plastic term of Eq. (24), which relaxes the stress back into the stable, convex region. Hence, although the imposed perturbation creates a local stress response along the direction associated with the negative eigenvalue initially, it is the stress relaxation back

[11] Note the difference in nomenclature: $T_G \sim T_g^2 \propto v_s^2$, see the text around Eq. (2).

to the convex region that dominates for finite times. If not strong/fast enough, the system will yield or un-jam dynamically. This is one way how GSH accounts for stability and un-jamming dynamics by instability, both mediated by the granular temperature

Unfortunately, including the elastic dissipative terms renders Eq. (24) an unstable partial differential equation, the solution of which requires increased technical efforts. This is undesirable in a first, qualitative study, and an approximation scheme may prove useful. We suggest to go on neglecting the elastic dissipative terms, and to add a stress term to Eq. (22), such that T_g is directly produced by an elastic stress.

The balance equations for s, s_g, for the energetically convex region, are given as

$$T\tfrac{\partial}{\partial t}s = R = \gamma T_g^2 + \beta_{ijkl}\pi_{ij}\pi_{kl} + \cdots\,, \tag{25}$$
$$T_g\tfrac{\partial}{\partial t}s_g = R_g = -\gamma T_g^2 + \eta_g v_{ij}v_{ij}. \tag{26}$$

The equally permissible alternative was not adopted,

$$T\tfrac{\partial}{\partial t}s = \gamma T_g^2 + \cdots\,, \tag{27}$$
$$T_g\tfrac{\partial}{\partial t}s_g = -\gamma T_g^2 + \eta_g v_{ij}v_{ij} + \bar\beta_{ijkl}\pi_{ij}\pi_{kl}, \tag{28}$$

because any static π_{ij} would then produce T_g, leading to its decay. This is not observed. Yet the reasoning is not valid outside the cone, where static stresses are not stable. Hence we combine Eq. (25) with (28), noting

$$\bar\beta_{ijkl} = 0 \text{ inside,} \quad \text{and } \beta_{ijkl} = 0 \text{ outside,} \tag{29}$$

the cone. The explicit form for $\beta_{ijkl}, \bar\beta_{ijkl}$ is a constitutive choice that will be given in the next section. In the notation of Eq(23), we have

$$b\rho\tfrac{\partial}{\partial t}T_g = -\gamma_1 T_g^* T_g + \eta_1 v_s^2 + \bar\beta_{ijkl}\pi_{ij}\pi_{kl}. \tag{30}$$

3 Granular solid hydrodynamics (GSH)

GSH is a continuum mechanical theory for granular media, set up in compliance with thermodynamics and conservation laws. GSH possesses the *state variables*:
(i) density, ρ, or volume fraction, $\phi = \rho/\rho_p$,
(ii) momentum density, $\rho v_i = 0$, neglected here,
(iii) elastic isotropic strain $\Delta = -u_{ll} = \varepsilon_v^e = \ln(\rho/\rho_J)$,
(iv) elastic deviatoric (shear) strain $u_s = \sqrt{2J_2^u}$,
(v) granular temperature $T_G \propto T_g^2$, and
(vi) temperature T, not used in the following,
with conventions and nomenclature given in Sec. 1.5.

The question is now if it is possible to catch the complex phenomenology at yielding, jamming, un-jamming, elasticity and loss of elasticity with a simple model that only knows about four state variables: ρ, Δ, u_s, and T_g.

For the sake of completeness, we first recollect the more complex, more complete classical GSH, as published in the previous years, in Sec. 3.1, before we reduce GSH to an over-simplified minimal model in Sec. 3.2, which will allow for a better understanding of the structure of GSH. Note that the nomenclature of classical GSH is applied in Sec. 3.1, whereas we switch to the positive compressive strain convention and nomenclature in Sec. 3.2.

3.1 About classical GSH

The complete equations of GSH may be found in Refs. [69,70], a simplified version in Ref. [71], from which we boil down to a minimalistic version in subsection 3.2, ignoring not only momentum density and gradients, but also the density dependence of most transport coefficients and parameters, since those represent constitutive assumptions, rather than basic theory. First, we discuss a few complications in the classical GSH nomenclature, that are not necessary for our present focus, but will become important if a more quantitative model is the goal, so that we keep them as reference for the sake of completeness.

3.1.1 The classical GSH constitutive model

The energy density has a thermal and an elastic part:

$$w = w_T + w_\Delta, \qquad w_T = s_g^2/(2\rho b)\,,$$
$$w_\Delta = \sqrt{\Delta}[2B(\rho)\Delta^2/5 + G(\rho)u_s^2], \quad B, G > 0\,, \tag{31}$$

with $P_\Delta \equiv \pi_{\ell\ell}/3$. This represents the first constitutive assumption at the core of classical GSH. In the following, we drop the ρ-dependence of B and G for convenience. (In previous GSH-publications, G was denoted as $\mathcal{A}$.). The elastic stresses are defined as the derivatives of w with respect to the elastic strain u_{ij}:

$$\pi_{ij} \equiv -\partial w/\partial u_{ij} = P_\Delta\delta_{ij} - \pi_s u_{ij}^*/u_s\,, \tag{32}$$
$$P_\Delta = \sqrt{\Delta}(B\Delta + Gu_s^2/2\Delta), \quad \pi_s = 2G\sqrt{\Delta}\,u_s\,, \tag{33}$$
$$4P_\Delta/\pi_s = 2(B/G)(\Delta/u_s) + u_s/\Delta\,, \tag{34}$$

which represents no constitutive assumption, but is just a consequence of Eq. (31). Like the elastic stress, being conjugate to the elastic strain, the granular temperature is conjugate to the granular entropy, which allows to define the thermal pressure, P_T, as the derivative of the thermal free energy with respect to volume, at constant T_g, as:

$$T_g \equiv \partial w_T/\partial s_g = s_g/\rho b\,, \quad \to \quad w_T = \rho b T_g^2/2\,, \tag{35}$$
$$P_T \equiv -\left.\frac{\partial[(w_T - T_g s_g)/\rho]}{\partial[1/\rho]}\right|_{T_g} = -\frac{\rho^2 T_g^2}{2}\frac{\partial b}{\partial\rho}\,, \tag{36}$$

where we note that the granular entropy is not needed, replaced by the density dependent function $b = b(\rho)$. The elastic energy w_Δ has been tested for: (1) static stress distributions in silos, sand piles, point loads on a granular sheet [110]; (2) incremental stress-strain relations from varying static stresses [111]; (3) propagation of elastic waves at varying stresses [112].

As already observed in Ref. [69], w_Δ is convex if:

$$u_s/\Delta \leq \sqrt{2B/G} =: g_e, \quad \text{or} \qquad \pi_s \leq P_\Delta \sqrt{2G/B} = 2/g_e \ . \tag{37}$$

Because the macroscopic friction, or yield limit, $\mu_0 := \sqrt{2G/B}$, is observed to be not (or only weakly) density dependent, at least for cohesionless granular media, the next constitutive model assumption used is: $G/B = const.$, and

$$B = B_0 \left[(\rho - \bar{\rho})/(\rho_{cp} - \rho)\right]^{0.15} , \tag{38}$$

where $B_0 > 0$ is a constant, and $\bar{\rho} \equiv \frac{1}{9}(20\rho_{\ell p} - 11\rho_{cp})$, with $\rho_{cp} - \rho_{\ell p} \approx \rho_{\ell p} - \bar{\rho}$. ($\rho_{cp}$ is the *random-close packing density*, the highest one at which grains may remain uncompressed, $\rho_{\ell p}$ is the *random-loose packing density*, the lowest one at which grains may stay static.) The expression for B was empirically constructed to account for three granular characteristics: (1) It provides concavity, for any density smaller than $\rho < \rho_{\ell p}$, and convexity between $\rho_{\ell p}$ and ρ_{cp}, ensuring the stability of elastic solutions in this region. (2) The density dependence of sound velocities, c (as measured by Hardin and Richart [113]), is well approximated by $c = \sqrt{\mathcal{B}/\rho} \approx \sqrt{B\Delta^{1/2}/\rho}$. (3) The slow divergence at ρ_{cp} mimicks the fact that the system is much stiffer for $\rho = \rho_{cp}$ than at loose packing $B(\rho = \rho_{\ell p})$. Comparing these constitutive assumptions for G and B with particle simulations is subject of ongoing work, but goes beyond the scope of this paper [12].

Finally, the function b was chosen as:

$$b = b_1/\rho + b_0 \left[1 - \rho/\rho_{cp}\right]^a , \tag{39}$$

with another small power law, $a \approx 0.1$, such that $P_T \approx w_T$ for $\rho \to 0$, and $P_T \approx w_T/(\rho_{cp} - \rho)$ for $\rho \to \rho_{cp}$, limits which reduces b to first or second term, respectively, for details see Refs. [73,115]. The thermal pressure is explicitly given by:

$$P_T = \frac{\rho^2 T_g^2}{2} \left[\frac{b_1}{\rho^2} + \frac{a b_0}{\rho_{cp}(1 - \rho/\rho_{cp})^{1-a}}\right] =: \rho g_p T_g^2 \ , \tag{40}$$

which defines the abbreviation $g_p = (\rho/2)\partial b/\partial \rho$, that also is set to constant in the following sections, which is only a good approximation for low densities, i.e., $g_p \approx b_1/2 \approx 1$.

3.1.2 The evolution equations

For completeness, we specify the evolution equations in the classical GSH nomenclature, where we note the sign conventions $\Delta = \varepsilon_v^e$, $u_{ij} = -\varepsilon_{ij}^e$ and $v_{ij} = -\dot{\varepsilon}_{ij}$, see Sec. 1.5. For the elastic strain one has:

$$\frac{\partial}{\partial t} u_{ij}^* = v_{ij}^* - \lambda T_g u_{ij}^*, \tag{41}$$

$$\frac{\partial}{\partial t} \Delta + v_{\ell\ell} = \alpha_1 u_{ij}^* v_{ij}^* - \lambda_1 T_g \Delta, \tag{42}$$

with α_1 as an off-diagonal Onsager coefficient, accounting for the Reynolds dilatancy. Mass and momentum conservation read:

$$\frac{\partial}{\partial t} \rho + \nabla_i(\rho v_i) = 0, \tag{43}$$

$$\frac{\partial}{\partial t} (\rho v_i) + \nabla_i(\sigma_{ij} + \rho v_i v_j) = -\rho g_i, \tag{44}$$

with the total stress: $\sigma_{ij} = \pi_{ij} + P_T \delta_{ij} - \eta_1 T_g v_{ij}^*$, with viscosity, $\eta_g = \eta_1 T_g$.

Finally, the evolution equation for T_g, with b as given by Eq. (35) and $T_g^* \equiv T_g + \gamma_0/\gamma_1 =: T_g + T_e$, is given by Eqs. (30).

The coefficients $\alpha_1, \gamma_0, \gamma_1, \eta_1$, and ρb are all functions of the state variables, especially the density, which would require many more constitutive assumptions, so that they are over-simplified and taken as constants in the following.

3.2 Minimal GSH type model for a material point

At the core of GSH, assuming a homogeneous representative volume, without convection, $\rho v_i = 0$ and gradients, $\nabla_i(...) = 0$, one has a postulated energy density,

$$w = w_e + w_T \ , \tag{45}$$

with an elastic and a dynamic, kinetic/granular contribution. The total stress is thus not an independent (state) variable, but can be abbreviated as

$$\begin{aligned} \sigma_{ij} &= \pi_{ij} + P_T \delta_{ij} + \sigma_{ij}^{\text{visc.}} \\ &=: P_\Delta \delta_{ij} + \pi_{ij}^* + \rho T_g^2 g_p \delta_{ij} + \chi \dot{\varepsilon}_v \delta_{ij} + \eta \dot{\varepsilon}_{ij}^* \ , \end{aligned} \tag{46}$$

---

[12] To account for the un-jamming transition at the random loose density, $\rho_{\ell p}$, a density dependence of B was seen as necessary in the classical GSH literature. To account for the virgin consolidation curve, higher order elastic strain terms in the elastic energy were proposed, with density dependent coefficients, see [69,114]. The Coulomb yield could be accounted for with no density dependence, as in Eq. (37). Since our illustrative examples are focused on the latter, hence B is set to constant in Secs. 5 and 6. A quantitative comparison with particle simulation data will show which assumptions or terms are really needed.

where the five terms represent isotropic and deviatoric elastic stresses, kinetic/granular stress (with an over-simplified $g_p = 1$, which should depend – at least – on density, see Eq. (40)), and isotropic and deviatoric viscous stresses, with viscosities $\chi = \eta_v$ and $\eta = \eta_s$, respectively.

3.2.1 The elastic stress

One can derive the elastic stress $\pi_{ij} = \partial w/\partial u_{ij}$, from the simplest (non-linear) elastic energy density:

$$w_e = \sqrt{\Delta}\left((2/5)B\Delta^2 + Gu_s^2\right) \quad \text{if } \Delta > 0 \ , \tag{47}$$

and $w_e = 0$ if $\Delta \leq 0$, with $u_s^2 = \varepsilon_{ij}^{e*}\varepsilon_{ij}^{e*}$, and B, G carrying the units of stress, while their possible dependencies on other state-variables (like density) are ignored in the rest of this study, for the sake of simplicity, without loss of generality. The isotropic elastic pressure (defined in $\mathcal{D}$ dimensions) is:

$$P_\Delta = \frac{\pi_{ll}}{\mathcal{D}} = \frac{\partial w_e}{\partial \varepsilon_v^e} = B\Delta^{3/2} + \frac{1}{2}Gu_s^2\Delta^{-1/2} =: \mathcal{B}_\Delta \Delta \,,$$

and the deviatoric elastic stress is:

$$\pi_{ij}^* := \frac{\partial w_e}{\partial \varepsilon_{ij}^{e*}} = 2G\Delta^{1/2}\varepsilon_{ij}^{e*} =: \mathcal{G}_\Delta \varepsilon_{ij}^{e*} \,,$$

implicitly defining the (Δ-dependent) bulk and shear secant moduli $\mathcal{B}_\Delta$ and $\mathcal{G}_\Delta$, which mimick a linear Δ- or ε_{ij}^{e*}-dependence of isotropic or deviatoric stress, respectively, not to be confused with the (true) tangent moduli $\mathcal{B}$, $\mathcal{G}$ and $\mathcal{A}$. The notation details and alternative definitions of the state variables $\varepsilon_v^e = \Delta$ and $\varepsilon_{ij}^{e*} = -u_{ij}^*$ are given in Sec. 1.5.

3.2.2 Simplest GSH equations and discussion

For a material point, in absence of gradients, using $\partial_t \sim \partial/\partial t \sim d/dt$, the evolution of density with strain rate:

$$\partial_t \rho = \rho \dot{\varepsilon}_v \tag{48}$$

has no free parameters. Here, positive strain-rate corresponds to compression and negative to extension, i.e., density increase and decrease, respectively; density can also be seen as the volume fraction, related to each other by the (constant) material density, i.e., $\phi = \rho/\rho_p$. Later, units will be chosen, such that $\rho_p = 1$.

In the evolution equation for the isotropic elastic strain:

$$\partial_t \Delta = \dot{\varepsilon}_v - \lambda_1 T_g \Delta + \alpha_1 \varepsilon_{ij}^{e*}\dot{\varepsilon}_{ij}^* \tag{49}$$

the *first term* couples elastic and total strain together, while the *second term* is relaxing Δ towards zero [13] – in case of finite T_g, with rate $\lambda_1 T_g$. The *third term* can be positive (or negative, e.g., at strain reversal) and thus works against (or with) the relaxation term, with rate $\alpha_1 v_s = \alpha_1|\dot{\varepsilon}_{ij}^*|$. [14]

The third equation defines the evolution of the deviatoric (shear) elastic strain

$$\partial_t \varepsilon_{ij}^{e*} = \dot{\varepsilon}_{ij}^* - \lambda T_g \varepsilon_{ij}^{e*} \ , \tag{50}$$

where the *first term* creates deviatoric elastic strain, co-linearly with the strain-rate, while the *second term* relaxes the deviatoric elastic strain, with rate λT_g. A dilatancy term analogous to the third in Eq. (49) is not required by the Onsager relation, but may be added for symmetry, as was done in Ref. [81].

The fourth equation represents the evolution of the granular temperature

$$\begin{aligned} \partial_t T_g &= -R_T T_g T_g^* + f_T(\dot{\varepsilon}_{ij}) \\ &= R_{T0}\left[-(1-r^2)T_g T_g^* + f_s^2\dot{\varepsilon}_{ij}^*\dot{\varepsilon}_{ij}^* + f_v^2\dot{\varepsilon}_v\dot{\varepsilon}_v\right] \end{aligned} \tag{51}$$

with the abbreviation for the dissipation rate $R_T = \gamma_1/(\rho b) = R_{T0}(1-r^2)$, proportional to the energy dissipation factor $(1-r^2)$, where r is the (effective) restitution coefficient. The energy creation terms are condensed into the tensor function $f_T(\dot{\varepsilon}_{ij})$, independent on r, so that one could split them off with two energy creation rates, $R_{T0}f_s^2 = \eta_s/(\rho b)$ and $R_{T0}f_v^2 = \eta_v/(\rho b)$, for shear and volumetric strain-rates, respectively.

3.3 Minimal elastic model with two variables

One could decompose the elastic stress and strain tensors into invariants (and their orientations). Under the assumption of fixed and co-linear tensor-eigensystems, and ignoring the third invariant for the sake of brevity, what remains are the isotropic and deviatoric stresses, $\sigma_\alpha = \{P_\Delta, \pi_s = \pi_s^*\}$, and elastic strains, $u_\alpha = \{\Delta, u_s =$

[13] Relaxation of $\Delta \to 0$, at fixed density, ρ, implies that the granular temperature (jiggling) causes the jamming density to relax as $\rho_J \to \rho$, in both jammed and un-jammed states, increasing and decreasing, respectively. A decrease (an increase) of the elastic strain, Δ, at fixed density, ρ, corresponds to an increase (a decrease) of the jamming density, ρ_J, see Ref. [53]. On the other hand, at fixed confining pressure, P, a jammed system, at finite, but small T_g (tapping) will develop to a state such that the elastic pressure, $P_\Delta = P - P_T \approx P$, remains constant; relaxation of Δ then corresponds to an increase of density, i.e., compaction.

[14] After large strain, one has a positive product, $\varepsilon_{ij}^{e*}\dot{\varepsilon}_{ij}^* > 0$, but at strain reversal the same term can be negative, for a while, until the elastic deviatoric strain reverts direction.

$u_s^*\}$, each as 2-tuple vectors, denoted by Greek indices. This provides the criteria for energy minima:

$$\delta^2 w = -\delta\pi_{ij}\delta u_{ij} = \delta\pi_\alpha \delta u_\alpha = \frac{\partial \pi_\alpha}{\partial u_\beta}\delta u_\alpha \delta u_\beta > 0. \tag{52}$$

Using the (positive) invariants yields the simple 2x2 Hessian matrix (for second order elastic work):

$$\frac{\partial^2 w_e}{\partial u_\alpha \partial u_\beta} = \frac{\partial \pi_\alpha}{\partial u_\beta} = \begin{pmatrix} \partial P_\Delta/\partial \Delta & \partial P_\Delta/\partial u_s \\ \partial \pi_s/\partial \Delta & \partial \pi_s/\partial u_s \end{pmatrix}$$
$$=: \begin{pmatrix} \mathcal{B} & \mathcal{A} \\ \mathcal{A} & \mathcal{G} \end{pmatrix} = \mathbf{C} \tag{53}$$

If it has only positive eigenvalues, the (elastic) energy w_e is a convex function of the elastic strain-invariants Δ and u_s. With other words, an elastic stability criterion is $\det(\mathbf{C}) = \mathcal{B}\mathcal{G} - \mathcal{A}^2 > 0$.

3.3.1 GSH with Hertzian type elasticity

In the special case of a Hertzian type elastic energy density, see Eq. (47), as typically used in the GSH literature [70], one has:
$\mathcal{B} = (3/2)B\Delta^{1/2} - (1/4)Gu_s^2\Delta^{-3/2} \neq \mathcal{B}_\Delta$,
$\mathcal{G} = 2G\Delta^{1/2}$, and $\mathcal{A} = G\Delta^{-1/2}u_s$.
With this, the stability condition, $\mathcal{B}\mathcal{G} - \mathcal{A}^2 > 0$, translates to

$$g_e^2 := 2B/G \geq (u_s/\Delta)^2 \ , \tag{54}$$

as previously shown in Eq. (12) in Ref. [71], and in Eq. (37) above, for elastic, static systems above jamming, for $\Delta > 0$, while $w_e = 0$ and thus $\det(\mathbf{C}) = 0$ for $\Delta \leq 0$.

3.3.2 Eigen-values and -vectors at elastic instability

First, we compute the eigen-values and -vectors from the matrix $\mathbf{C}$, before we introduce constitutive assumptions and discuss those separately in the next subsubsections.

Basic linear algebra yields the two eigen-values, $C_{1,0} = (\mathcal{B}+\mathcal{G})/2 \pm \sqrt{(\mathcal{B}-\mathcal{G})^2/4 + \mathcal{A}^2}$, as solution of the quadratic equation $0 = (\mathcal{B} - C)(\mathcal{G} - C) - \mathcal{A}^2 = C^2 - C(\mathcal{B}+\mathcal{G}) + \mathcal{B}\mathcal{G} - \mathcal{A}^2$, with $C_1 = \mathcal{B}+\mathcal{G}$ and $C_0 = 0$, at the point of instability, where $\mathcal{B}\mathcal{G} = \mathcal{A}^2$.

Using C_1, and $\mathcal{A} = \sqrt{\mathcal{G}\mathcal{B}}$, with the two equations $-\mathcal{G}\hat{n}_1^{(1)} + \mathcal{A}\hat{n}_2^{(1)} = 0$ and $\mathcal{A}\hat{n}_1^{(1)} - \mathcal{B}\hat{n}_2^{(1)} = 0$, results in the corresponding eigen-vector (with $\hat{n}_2^{(1)} = \hat{n}_1^{(1)}\mathcal{G}/\mathcal{A} = \hat{n}_1^{(1)}\mathcal{A}/\mathcal{B} = \hat{n}_1^{(1)}\sqrt{\mathcal{G}/\mathcal{B}}$), which defines the "direction" (in elastic strain invariants) of maximal stability: $\hat{n}^{(1)} = \pm(1, \sqrt{\mathcal{G}/\mathcal{B}})/\sqrt{1+\mathcal{G}/\mathcal{B}}$

Using $C_0 = 0$, and $\mathcal{A} = \sqrt{\mathcal{G}\mathcal{B}}$, with the two equations $\mathcal{B}\hat{n}_1^{(0)} + \mathcal{A}\hat{n}_2^{(0)} = 0$ and $\mathcal{A}\hat{n}_1^{(0)} + \mathcal{G}\hat{n}_2^{(0)} = 0$, results in the corresponding eigen-vector (with $\hat{n}_2^{(0)} = -\hat{n}_1^{(0)}\mathcal{B}/\mathcal{A} = -\hat{n}_1^{(0)}\mathcal{A}/\mathcal{G} = -\hat{n}_1^{(0)}\sqrt{\mathcal{B}/\mathcal{G}}$), which gives the "direction" of instability (in the space of elastic strain-invariants): $\hat{n}^{(0)} = \pm(-\sqrt{\mathcal{G}/\mathcal{B}}, 1)/\sqrt{1+\mathcal{G}/\mathcal{B}}$, perpendicular to the direction of maximal stability. Note the special role the ratio of shear to bulk modulus takes in this analysis.

More explicitly, incremental changes in the elastic strain, $\delta u_\alpha = (\delta\Delta, \delta u_s) = \delta\varepsilon^e\, \hat{n}_\alpha^{(0)}$, at the point of elastic instability, can be done without any change of elastic energy, $\delta^2 w = (\delta\varepsilon^e)^2 \hat{n}_\alpha^{(0)}\hat{n}_\beta^{(0)} C_{\alpha\beta} = 0$, and are thus permitted from energy/thermodynamic arguments. With other words, any other elastic strain increment will require energy to be realized. For energy considerations, see also Ref. [55,58] and references therein.

3.3.3 Hertzian elastic energy instability

The non-zero eigenvalue can be re-written, using the choice for w_e in Eq. (47), as: $C_1 = [B + 2G]\Delta^{1/2} = B[1 + 4/g_e^2]\Delta^{1/2}$, with $g_e = \sqrt{2B/G}$, while the zero eigenvalue will be more relevant for understanding the failure mechanism.

Using w_e in Eq. (47), this translates to the eigen-vectors: $\hat{n}^{(1)} = \pm(g_e, 1)/\sqrt{1+g_e^2}$, and $\hat{n}^{(0)} = \pm(1, -g_e)/\sqrt{1+g_e^2}$. More explicitly, incremental changes in the elastic strain, $\delta u_\alpha = (\delta\Delta, \delta u_s) = \delta\varepsilon^e\, \hat{n}_\alpha^{(0)}$, at the point of elastic instability, can be done without any change of elastic energy, $\delta^2 w = (\delta\varepsilon^e)^2 \hat{n}_\alpha^{(0)}\hat{n}_\beta^{(0)} C_{\alpha\beta} = 0$, and are thus permitted.
In a shear to normal stress space, one could see the limit of elasticity as one possible definition of the maximal (elastic) macroscopic (bulk) friction, with bulk friction defined by the ratio: $\mu_e := \pi_s^*/P_\Delta = \mathcal{G}_\Delta u_s/(\mathcal{B}_\Delta \Delta)$, with the limit value taken at the loss of elastic stability: $\mu_e^0 = \sqrt{2G/B} = 2/g_e$.

3.3.4 Anisotropic, linear elastic energy instability

In Ref. [81], the elements of the constitutive matrix $\mathbf{C}$ were directly deduced from particle simulations, and took a form (slightly simplified here by implying that the fabric and the elastic strain are proportional): $\mathcal{B} = B_0\phi Z$ (with the product of volume fraction ϕ and coordination number Z, which is a non-linear function of Δ), $\mathcal{G}/\mathcal{B} = G_0(\Delta)(1 - u_s^2)$, and $\mathcal{A}/\mathcal{B} = u_s$.
From this, the condition for elastic instability translates to: $(u_s^e)^2 = G_0(\Delta)/(1 + G_0(\Delta))$, which implies a very narrow but steep elastic regime for small Δ, since $G_0(\Delta) = (1/2)(1 - \exp(-\Delta/\Delta_g)) \to (1/2)\Delta/\Delta_g$, vanishes for $\Delta \to 0$, so that $u_s^e \propto \sqrt{\Delta}$. For large $\Delta/\Delta_g \gg 1$, one has instead $u_s^e \approx 1/3$, independent of Δ.

The "direction" (in elastic strain invariants) of maximal stability becomes: $\hat{n}^{(1)} = \pm(1, \sqrt{\mathcal{G}/\mathcal{B}})/\sqrt{1+\mathcal{G}/\mathcal{B}} = \pm(1, u_s)/\sqrt{1+u_s^2}$, and with the perpendicular "direction" of maximal in-stability: $\hat{n}^{(0)} = \pm(-\sqrt{\mathcal{G}/\mathcal{B}}, 1)/\sqrt{1+\mathcal{G}/\mathcal{B}} = \pm(-u_s, 1)/\sqrt{1+u_s^2}$, after using $\sqrt{\mathcal{G}/\mathcal{B}} = \mathcal{A}/\mathcal{B} = u_s$.

3.4 Special cases

In order to understand what the eigen-vectors mean, it is instructive to consider a few simple special cases. Some of these cases are later studied analytically and numerically. They represent simplifications that boil down a complicated theoretical framework to a simpler, possibly even transparent form that allows for better understanding and sometimes even for analytical solutions. We propose to apply those special cases to any new theory before one really applies the whole framework. Furthermore, the special cases allow to isolate a few of the terms and possibly calibrate the model parameters one by one.

For the rest of this section, we use the results from the Hertz-like elastic energy density, as discussed in subsection 3.3.3. Most of the cases are illustrated schematically in Fig. 2.

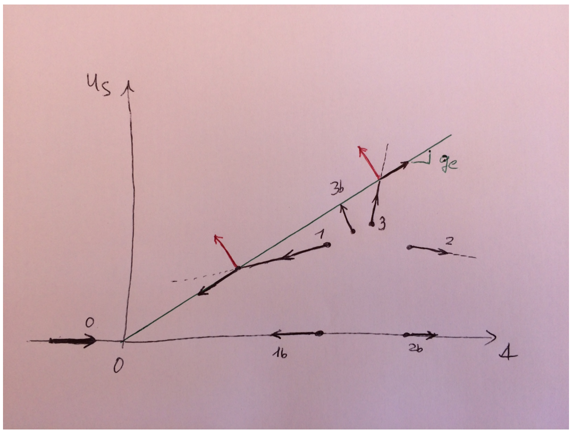

Fig. 2 Sketch of the (strain-rate driven) deformation cases in the space of the elastic strain invariants, i.e., u_s plotted against Δ. The numbers at the black arrows indicate the case-number, where dashed, thin lines are not allowed, continuing the trends in the permitted zone. The red arrows give the eigen-vector of instability $\hat{n}^{(0)}$.

Except for the first case 0, the following cases start from a jammed, elastically stable state with finite initial elastic strains $\Delta(0) > 0$ and $u_s(0) > 0$.

(case 0) Assume the system unjammed, $\Delta(0) < 0$, and apply a constant compressive strain-rate, $\dot{\varepsilon}_v = -v_{ll} > 0$. The density and the elastic strain, $\Delta = \log(\rho/\rho_J)$, will grow together until the system jams at ρ_J, from which on its evolution equation kicks in. It was shown in Refs. [116,117], and earlier works cited therein, that already below jamming, the jamming density (and thus Δ) depends on the procedure of preparation, in particular on the strain-rate and on the granular temperature, however, this fact goes beyond the present focus and is thus ignored here.

(case 1) Assuming a purely isotropic de-compression, $\dot{\varepsilon}_v = -v_{ll} < 0$, from a jammed state, one expects the elastic isotropic strain, Δ, to decrease faster than its deviatoric (shear) counterpart, u_s, until at $u_s^2 = (2B/G)\Delta^2$, or $u_s = g_e\Delta$, the system cannot sustain the applied shear-stress anymore, so that un-jamming due to instability with respect to shear occurs. In order to remain at least marginally stable, one needs a decrease of $u_s \to u_s^0 = g_e\Delta$, a situation that could be referred to as shear-yielding [39,44,53].

(case 1b) In the situation without initial elastic shear strain, $u_s(0) = 0$, the stability criterion is always true and the system remains stable until isotropic un-jamming takes place at $\Delta = 0$.

(case 2) In the case of isotropic compression, the model remains stable, unless the virgin consolidation line is reached, where the system restructures to be able to carry the increasing stress.

(case 3) Assuming a purely deviatoric (volume conserving) shear strain rate, $\dot{\varepsilon}^*_{ij} = -v^*_{ij}$, from a state with initial $\Delta > 0$, one expects the elastic deviatoric (shear) strain, u_s, to increase faster than its isotropic counterpart, Δ, could build up, until at $\Delta = u_s/g_e$, the system cannot sustain pressure (isotropic stress) anymore, so that an instability with respect to volume change occurs, and one has a consequent increase of $\Delta \to \Delta^0 = u_s/g_e$, which can be seen as one origin of dilatancy. However, the evolution of Δ is changing qualitatively, when the limit of elastic stability is reached, as will be studied numerically later on.

(case 3b) Under the same purely deviatoric deformation, the isotropic elastic strain Δ could also decrease, which only leads to instability at smaller elastic strains, not much changing the considerations in case 3, but rather leading to compactancy.

Several of the cases discussed above will be now studied analytically (as far as possible) and numerically.

4 Analytical results for special cases

This section considers first the athermal limit, $T_g = 0$, before granular temperature is included into the equations and various versions of the model are discussed. Finally, two regularization schemes are proposed, to be later used for the numerical solutions. But first we summarize the equations that will be used in this section.

The set of model equations is summarised here for reference, with the colored terms representing extensions from the black terms (representing model 0):

$$\partial_t \rho = \rho \dot{\varepsilon}_v \tag{55}$$
$$\partial_t \Delta = \dot{\varepsilon}_v (1 - p_v) - \lambda_1 T_g \Delta p_g + \alpha_1 \varepsilon^{e*}_{ij} \dot{\varepsilon}^*_{ij} (1 - p_s) \tag{56}$$
$$\partial_t \varepsilon^{e*}_{ij} = \dot{\varepsilon}^*_{ij} (1 - p_s) - \lambda T_g \varepsilon^{e*}_{ij} + \alpha_d \tag{57}$$
$$\partial_t T_g = -R_T T_g^2 (T_g^*/T_g) + f_T(\dot{\varepsilon}_{ij}) + f_g(g^*) \ , \tag{58}$$

before some meaningful special cases (isotropic and deviatoric loading) are discussed below, for which analytical solutions are provided, if possible. The colored terms are not present in the original Eqs. (48)-(51), which is referred to as model 0, having thus no valid athermal limit.

The blue terms p_g and α_d are introduced here as place-holders for elements discussed below, in subsection 4.6, or to be added in future, introduced in Refs. [118,81,53]. The rate of cooling is modified in the elastic, jammed state ($\Delta > 0$) by adding an "elastic dissipation rate" T_e, referred to as model e, as $T_g^*/T_g = 1 + T_e/T_g = 1 + T_{e0}\Delta^h/T_g$ where only the special case $h = 0$, i.e., $T_e = T_{e0}$, will be treated below [15]. The presence of T_e does not affect the dynamics too much for large T_g (for more details, see below), but in the limit of very small $T_g \to 0$, for elastic, jammed systems, this (phonon/wave-driven) dissipation becomes important, providing an exponential decay of $T_g \to 0$ in absence of other driving mechanisms (and constant $\Delta > 0$).

The new magenta term $f_g(g^*) = f_g^2(g^*)^2\theta(g^*)$, in Eq. (58), is only active if the system is outside of the elastically stable regime, where $g^* = u_s/\Delta - g_e > 0$, with the limit of elastic stability g_e, and the step-function $\theta(x \geq 0) = 1$, or $\theta(x < 0) = 0$. This term generates more granular temperature, jiggling, due to concavity of the elastic energy, the more the system gets elastically unstable.

The terms $(1 - p_v)$ and $(1 - p_s)$ represent the probabilities for elastic deformations, with p_v and p_s the probabilities for isotropic/deviatoric plastic deformations, respectively, see Ref. [53], as specified in Sec. 2.1, and discussed next, in section 4.1.

4.1 The granular athermal limit $T_g = 0$

Enforcing the athermal case, $T_g = 0$, the system of equations reduces to:

$$\partial_t \Delta = \dot{\varepsilon}_v (1 - p_v) + \alpha_1 \varepsilon^{e*}_{ij} \dot{\varepsilon}^*_{ij} (1 - p_s) \ , \tag{59}$$
$$\partial_t \varepsilon^{e*}_{ij} = \dot{\varepsilon}^*_{ij} (1 - p_s) \ , \tag{60}$$

where the off-diagonal Onsager coefficients p_v and p_s were introduced in Ref. [69] and taken equal to α_1. Alternatively, they were interpreted in Refs. [53,118] as the probabilities for (isotropic and deviatoric) plastic (re-structuring) events in the packing. Note that in Eqs. (59) and (60), the probabilites for isotropic and deviatoric plastic deformations are attached to isotropic and deviatoric strain-rates, respectively.

4.1.1 Athermal isotropic loading

For *isotropic loading* ($\dot{\varepsilon}^*_{ij} = 0$), the system reduces even further to $\dot{\varepsilon}^p_v := \dot{\varepsilon}_v - \partial_t \Delta = \dot{\varepsilon}_v p_v$, or [16] one has: $\partial_t \ln(\rho_J) = \dot{\varepsilon}_v p_v$. In the elastic limit, with probability $p_v = 0$, this translates to constant Δ, whereas the fully plastic limit, $p_v = 1$, translates to $\dot{\varepsilon}^p_v = \dot{\rho}/\rho = \dot{\varepsilon}_v$. In all other cases, the probability for plastic deformations should be a function of the state-variables and the sign of deformation rate (i.e., compression or tension).

A simple constitutive assumption, $p_v \dot{\varepsilon}_v = -\lambda_1 T_e \Delta$, could be directly merged into the relaxation term as $-\lambda_1 T_g^* \Delta$, with $T_g^* = T_g + T_e$, and solved analytically [17]. This model displays the transient elastic behavior of polymer melts or glasses for which (in absence of any isotropic strain rate) $\Delta \to 0$. However, since the reality of granular matter, as measured from particle simulations in Ref. [53], is somewhat more complex, already for frictionless spheres – and even more for realistic frictional non-spherical particles – we have to come up with a better relation for the probability for isotropic plastic rearrangements.

The probability for plastic deformations was reported in Ref. [53], as $p_v^\Delta \propto \Delta/\Delta_\infty$, with the limit elastic strain, $\Delta_\infty = \ln(\rho/\rho_\infty)$, expected to be reached after infinitely many isotropic loading/un-loading cycles up to density ρ, with the corresponding density:

$$\rho_\infty = \rho_{J0} + b_\infty \left[\frac{\rho}{\rho_{J0}} - 1 \right]_+^{\beta_\infty} \ , \tag{61}$$

with the half-sided linear function $[x > 0]_+ = x$, and $[x \leq 0]_+ = 0$, otherwise, guaranteeing $\rho_\infty = \rho_{J0}$ for

[15] For a Hertzian type bulk modulus, the time-scale of momentum (wave) propagation, for $u_s = 0$, can be estimated as $t_e = 1/T_e = d/v_e \propto d/\sqrt{\mathcal{B}_\Delta/\rho} = d\sqrt{\rho/B\Delta^{1/2}} \propto \Delta^{-1/4}$, i.e., an exponent $h = 1/4$. This estimate, together with a Hertzian elastic pressure, $P_\Delta \propto \Delta^{3/2}$, yields an estimated wave speed $v_e \propto P_\Delta^{1/6}$ or moduli $\mathcal{B} \propto P_\Delta^{1/3}$.

[16] By using the chain rule, one has: $\partial_t \Delta = (\partial_t \rho)/\rho - (\partial_t \rho_J)/\rho_J = \dot{\varepsilon}_v - \partial_t \ln(\rho_J)$, as input.

[17] Inserting the expression from above, this yields the athermal evolution of the elastic strain: $\dot{\Delta} = v_{ll} - \lambda_1 T_{e0} \Delta^{1+h}$.

$\rho < \rho_{J0}$. The density ρ_{J0} represents the random loose packing density, i.e., the lowest possible isotropic jamming density, related to e_0, as discussed in section 1. The density ρ_∞ is the density for which the system would isotropically jam/un-jam, where the subscript indicates infinitely long relaxation. [18]

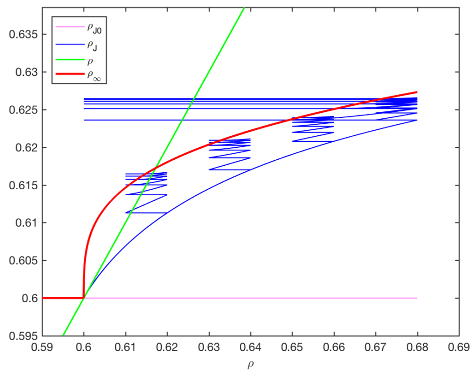

Fig. 3 Jamming density $\rho_J = \rho \exp(-\Delta)$, plotted against density, ρ, during loading up to $\rho_{max} = 0.62$, 0.64, 0.66, and 0.68, with subsequent un-/re-loading cycles with amplitude, $\delta\rho = 0.01$. The horizontal blue lines on top correspond to $\rho_{max} = 0.68$ and $\delta\rho = 0.08$. The solid red line represents ρ_∞ in Eq. (61), with $\rho_{J0} = 0.6$, and coefficients $p_{v0} = 1$, $b_\infty = 0.05$, $\beta_\infty = 0.30$. Note the flat blue lines for un-loading and for $\rho_J < \rho_\infty$, i.e., cases where one has $p_v = 0$.

For the sake of simplicity, in the numerical solution of the evolution equations, we implemented the simpler plastic deformation rate: $\dot{\varepsilon}_v p_v = p_{v0} \max(\dot{\varepsilon}_v, 0)(\rho_\infty - \rho_J)/(\rho_\infty - \rho_{J0})$, with $p_{v0} = 1$, according to Kumar and Luding, 2016 [53], idealized to be active for compression only, which yields qualitatively similar results, with a rather rapid approach to the maximal jamming density ρ_∞, while the above model $\dot{\varepsilon}_v p_v^\Delta$, with a much slower approach (stretched exponential) to ρ_∞, will be detailed elsewhere. The evolution of the jamming density and of pressure with density during initial loading and cyclic un-/re-loading are plotted in Figs. 3 and 4, to illustrate the phenomenology, including un-jamming/jamming, with details of the (numerical) model given in the next Sec. 5.

[18] Thus, ρ_∞ takes the place of the random close packing density, ρ_{cp}, but continuously grows with density. The high densities could be achieved (by over-compression) of soft particles (rubber, gel, etc.), whereas hard particles (metal, glass, etc.) would break (not considered here). For hard particles, one could replace Eq. (61) with a step function equal to ρ_{cp} for $\Delta > 0$.

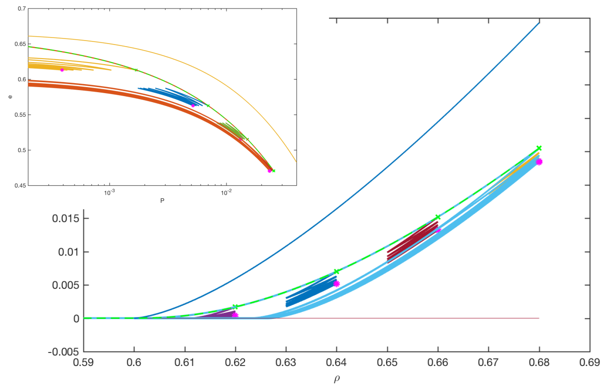

Fig. 4 Pressure plotted against density, from the same model solution as in Fig. 3. The lower curve represents the initial loading, up to ρ_{max} (green dots), with six cyclic un-/re-loading cycles, ending at the magenta dots. Note that the lowermost case with $\rho_{max} = 0.62$ is un-jamming and jamming during the cycles for several times. The upper curve represents the elastic limit case, with $p_v = 0$, i.e., with no plastic rearrangements and the analytical pressure state-line: $P_\Delta = B\Delta^{3/2}$, with $B = 1$, for details see Sec. 5. The lowermost curves represent cyclic un-/re-loading from $\rho_{max} = 0.68$ with amplitude $\delta\rho = 0.08$, well below the jamming-point. The inset represents the void fraction e plotted against (logarithmic) P, similar to Fig. 1-a.

4.1.2 Athermal deviatoric loading

For purely *deviatoric (isochoric) shear*, $\dot{\varepsilon}_v = 0$, the elastic shear strain develops as $\partial_t \varepsilon_{ij}^{e*} = \dot{\varepsilon}_{ij}^{*}(1 - p_s)$ or, equivalently, for the plastic strain rate $\dot{\varepsilon}_{ij}^{p} = \dot{\varepsilon}_{ij}^{*} - \partial_t \varepsilon_{ij}^{e*} = \dot{\varepsilon}_{ij}^{*} p_s$. Postulating the existence of a constant "critical" steady state for the stress ratio $\mu_0^c := \mu^c(v_s \to 0) = \mathcal{G}^c u_s^c/(\mathcal{B}_\Delta^c \Delta^c)$ [19], this allows to express the probability for plastic (shear) events as:

$$p_s = \frac{\mu}{\mu_0^c} = \frac{\left[\varepsilon_{ij}^{e*}\dot{\varepsilon}_{ij}^{*}\right]_+}{u_s^c v_s} \approx \frac{u_s}{u_s^c} \,, \tag{62}$$

where the last approximation is only valid after sufficiently long steady shear, close to the critical state, but not for strain reversal. The term in brackets is limited to keep it a probability, i.e., $[x > 0]_+ = x$, and $[x \le 0]_+ = 0$, and thus also valid for strain-reversal, as done similarly in Ref. [53,118,81] and references therein – based on, and in quantitative agreement with, DEM simulations [20]. The probability for plastic events in Eq.

[19] This implies a relation $\mathcal{G}_\Delta^c/\mathcal{B}_\Delta^c = \mu_0^c \Delta^c/u_s^c = 2G/[B + (1/2)G(u_s^c/\Delta^c)^2] = 4/[g_e^2 + (u_s^c/\Delta^c)^2]$ between shear and bulk modulus, and allows to determine from the quadratic equation: $\mu_0^c(u_s^c/\Delta^c)^2 - 4u_s^c/\Delta^c + \mu_0^c g_e^2 = 0$ the shear to isotropic elastic strain ratio $u_s^c/\Delta^c = 2/\mu_0^c \pm \sqrt{(2/\mu_0^c)^2 - g_e^2}$, with real solutions for $\mu_0^c \le 2/g_e$, as realized in cases modelled here (data not shown).

[20] If one can assume: $\Delta \approx \Delta^c$, i.e., that the isotropic elastic strain is almost constant, close to its critical state limit already, Eq. (60) can be solved analytically, yielding an ex-

(60) is finite, but very small, at the beginning of shear with build-up of elastic shear strain, u_s, but asymptotically approaches $p_s = 1$ for large strain in the perfectly plastic, critical state. At reversal of shear, the argument of the bracket-function becomes negative, i.e., the system is elastic with $p_s = 0$, until the shear strain is built up sufficiently in the new direction [21].

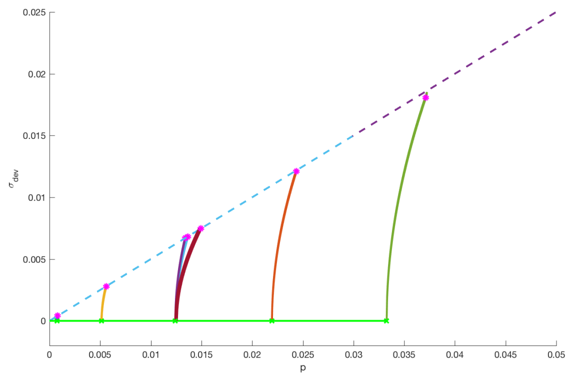

Fig. 5 Shear stress, $\sigma_{\rm dev} := \sigma_s$, plotted against pressure, P, from simulations compressed up to $\rho_{max} = 0.61$, 0.63, 0.65, 0.67, and 0.69 (green dots), and subsequent cyclic pure shear with amplitude, $\delta\gamma \sim 0.28$, where the magenta dots represent the end-situation after six forward-backward shear cycles. The dashed line indicates the pre-set slope $\mu_0^c = \sigma^c_{\rm dev}/P^c = 0.5$. The only other parameter active in this model is $\alpha_1 = 2$, where the case $\rho_{max} = 0.65$ was simulated with two other values of $\alpha_1 = 0.5$ and 8, to display the enhancing effect on pressure-dilatancy of this parameter. Note that the imposed maximal macroscopic friction, here, is chosen smaller than the elastic stability limit, $\mu_0^c < 2/g_e = 1$, such that the latter is never reached.

Noting the similarity between p_s and the α_1-term, one can rewrite the evolution equation for the isotropic elastic strain as: $\dot{\Delta} = \alpha_1 u_s^c v_s p_s (1 - p_s) \approx \alpha_1 u_s v_s (1 - p_s) = \alpha_1 u_s \dot{u}_s$, for constant v_s (not valid for strain-reversal). This equation has a critical state solution, Δ^c, due to the term $(1 - p_s)$, as well as a stable elastic solution with $\dot{\Delta} = 0$ for $p_s \approx 0$, see the infinite slopes in Fig. 5 for small shear strain and thus small shear stress. The deviatoric elastic strain evolves as $\dot{u}_s = v_s(1 - p_s) \approx v_s(1 - u_s/u_s^c)$, with analytical solution:

$$u_s(t) = u_s^c - [u_s^c - u_s(0)] \exp(-v_s t / u_s^c) \ , \tag{63}$$

with $u_s^c = \Delta \left[2/\mu_0^c - \sqrt{(2/\mu_0^c)^2 - g_e^2} \right]$, as plotted in the inset of Fig. 5 as shear stress evolution $\pi_s^* = 2G\Delta^{1/2} u_s$.

ponential approach of u_s to its critical state limit, see Ref. [53].

[21] Like for p_v, this could be merged into the relaxation term $-\lambda T_g^* u_{ij}^*$, if one would assume: $-v_{ij}^* p_s = -\lambda T_e u_{ij}^*$, the discussion of which goes far beyond this paper.

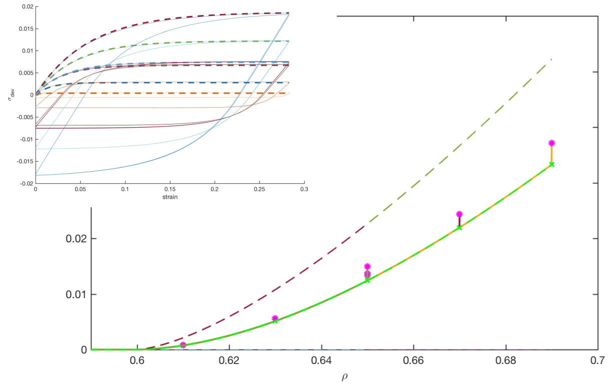

Fig. 6 Pressure plotted against density, from the same model solution as in Fig. 5. The lower curve represents the initial loading, up to ρ_{max} (green dots), with six cyclic forward-backward shear cycles, ending at the magenta dots, displaying the pressure-dilatancy caused by shear. The upper curve represents the elastic limit compression, with $p_v = 0$. The inset represents the shear stress evolution with strain, during the cyclic forward-backward shearing, where the higher density cases reach larger stress levels, and the dashed lines represent the analytical solutions from Eq. (63).

This analytical solutions are very similar in form to those used in Refs. [53,118], however, further discussion is beyond the scope of this paper [22].

4.2 The granular thermal limit $\dot{T}_g = 0$

Assume that one could maintain a constant granular temperature, which would result in the set of equations:

$$\partial_t \Delta = \dot{\varepsilon}_v (1 - p_v) - \lambda_1 T_g \Delta p_g + \alpha_1 \varepsilon_{ij}^{e*} \dot{\varepsilon}_{ij}^* (1 - p_s) \tag{64}$$

$$\partial_t \varepsilon_{ij}^{e*} = \dot{\varepsilon}_{ij}^* (1 - p_s) - \lambda T_g \varepsilon_{ij}^{e*} \ . \tag{65}$$

For vanishing strain-rate $\dot{\varepsilon}_{ij} = 0$, the equations decouple and only the relaxation terms survive, This corresponds to the "plastic equilibrium" limit case $\Delta = 0$, $\varepsilon_{ij}^{e*} = 0$, which is approached exponentially fast, with rates $\lambda_1 T_g$ and λT_g. The term $p_g = 1$ allows to choose the plastic equilibrium of transiently elastic systems, for which $\Delta \to 0$, or in a form $p_g = 1 - \Delta_\infty/\Delta$, the granular plastic limit with $\Delta > 0$, see subsection 4.6.

For finite $\dot{\varepsilon}_{ij}$, the system will establish thermal, elasto-plastic dynamic states that are not discussed further for the sake of brevity.

Strictly controlling density, i.e., fixing e, the situation is interesting again for granular matter. Any perturbation, as tapping or small-amplitude cyclic shear, will typically result in a decrease of both the elastic strain, Δ, and consequently the pressure, $P_\Delta = \mathcal{B}_\Delta \Delta$,

[22] Note that since u_s^c depends (weakly) on Δ, the system of equations is still coupled and the analytical solution is only approximate.

with elastic bulk-modulus $\mathcal{B}_\Delta = B\Delta^{3/2}$. In this situation, the pressure curve shifts to smaller densities (larger e), and changes slope, both moving it away further from the elastic state-line (not shown here). On the other hand, large strain shear results in (pressure) dilatancy, shifting the state-line to the right, towards the VCL (but not beyond), defining the critical state line (CS) – see Fig. 6.

4.3 Isotropic jamming in a minimal GSH

The model equations for isotropic compression/tension, with strain rates $\partial_t\rho = \dot\varepsilon_v \neq 0$, and $\dot\varepsilon^*_{ij} = 0$, reduce to:

$$\partial_t\Delta = \dot\varepsilon_v(1-p_v) - \lambda_1 T_g \Delta \tag{66}$$
$$\partial_t\varepsilon^{e*}_{ij} = -\lambda T_g \varepsilon^{e*}_{ij} \tag{67}$$
$$\partial_t T_g = -R_T T_g^2 (T^*_g/T_g) + f_T(\dot\varepsilon_{ij}) + f_g(g^*) \tag{68}$$

The density is coupled to strain-rate directly, while the second equation (67) is decoupled (just relaxing an existing elastic shear strain to zero). From the coupled evolution equations (66) and (68) for Δ and T_g, we observe that the situation at the end of an isotropic compression is independent of the density reached if $p_v = 0$. of the evolution of Δ and could be (quantitatively) calibrated to the numerical data in Ref. [53] in a future study. The energy production term due to elastic instability in Eq. (68) would become active for finite u_s, when $\Delta < g_e u_s$, but is ignored here, assuming $u_s = 0$ (which is not strictly true in real systems, where there can be some small, random elastic deviatoric strain).

The evolution equation for T_g, abbreviating $\gamma = R_T = R_{T0}(1-r^2)$, and assuming $T_e = 0$, results in an algebraic evolution:

$$\frac{T_g}{T_g^0} = \frac{1}{1+R_T T_g^0 t} \ , \tag{69}$$

in the free, homogeneous cooling state, as relevant for systems below jamming in the granular gas state. On the other hand, assuming the simplest model for $T^*_g \approx T_e$, with $h = 0$ (or for constant Δ), for a small perturbation from an elastic base state, one has

$$\frac{T_g}{T_g^0} = \exp\left(-R_T T_e t\right) \ , \tag{70}$$

as relevant for elastically stable systems, well above the jamming density, for which small perturbations decay exponentially fast.

For finite positive (compressive) strain-rate, the inhomogeneous solution leads to a divergent increase of T_g with time due to the continuous energy input. For negative (expansive) strain-rate, the same is true, however, as soon as the system isotropically un-jams, the behavior should qualitatively change – which is not accounted for in the present version with constant parameters, in particular f_v and R_{T0}; more details are beyond the scope of this study.

4.4 Pure shear from an isotropic state

This case was studied in detail by particle simulations in Refs. [81,53], and should be studied analytically too with respect to questions about the build-up of anisotropy, and the degradation of moduli, but is skipped for the sake of brevity.

4.5 Steady state pure shear (model 0 and e)

In case of deviatoric pure shear, the density equation vanishes, since $v_{ll} = 0$ the density is conserved, $\partial_t\rho = 0$, and the terms with isotropic strain rate in the equations drop out. The remaining equations yield the steady state solution for the granular temperature:

$$\partial_t T_g = 0 = R_{T0}\left[-(1-r^2)T_g T^*_g + f_s^2 \dot\varepsilon^*_{ij}\dot\varepsilon^*_{ij}\right]$$

with $T^*_g = T_e + T_g$, so that (for $T_e = 0$):

$$(T_{g0}^{(ss)})^2 = \frac{f_s^2(\dot\varepsilon^*_{ij}\dot\varepsilon^*_{ij})}{(1-r^2)} = \frac{f_s^2 v_s^2}{(1-r^2)} \ , \tag{71}$$

or (for $T^*_g = T_g + T_e$):

$$(T_g^{(ss)})^2 + T_g^{(ss)} T_e - (T_{g0}^{(ss)})^2 = 0 \ ,$$

yields

$$T_g^{(ss)} = \pm\sqrt{(T_e/2)^2 + (T_{g0}^{(ss)})^2} - T_e/2 \ , \tag{72}$$

where only the positive solution is reasonable.

In the "collisional" limit $T_g \gg T_e$, one has the dynamic steady state: $T_g^{(ss)} \approx T_{g0}^{(ss)} \propto v_s$, while for $T_g \ll T_e$, the steady state temperature in the "elastic" steady state is: $T_{ge}^{(ss)} \approx (T_{g0}^{(ss)})^2/T_e \propto v_s^2$, i.e., it vanishes quadratically for $v_s \to 0$.

For the deviatoric elastic strain one has:

$$\partial_t\varepsilon^{e*}_{ij} = 0 = \dot\varepsilon^*_{ij} - \lambda T_g \varepsilon^{e*}_{ij} \ ,$$

so that:

$$u_s^{(ss)} = v_s/(\lambda T_g^{(ss)}) \text{ and } u_{s0}^{(ss)} = \sqrt{1-r^2}/(\lambda f_s) \ , \tag{73}$$

while for the isotropic elastic strain one has:

$$\partial_t\Delta = 0 = -\lambda_1 T_g \Delta + \alpha_1 \varepsilon^{e*}_{ij}\dot\varepsilon^*_{ij} \ ,$$

so that inserting Eqs. (71) and (73) yields the isotropic elastic strain in steady state:

$$\Delta^{(ss)} = \frac{\alpha_1 v_s^2}{\lambda_1 \lambda (T_g^{(ss)})^2} \text{ and } \Delta_0^{(ss)} = \frac{\alpha_1 (1-r^2)}{\lambda_1 \lambda f_s^2} , \qquad (74)$$

the former valid for model e, the latter for the simplest model 0, where the subscript 0 indicates $T_e = 0$; model e is not indicated since it represents the default case.

In the "elastic" limit $T_g \ll T_e$, for $v_s \to 0$, the other two state variables, in model 0, behave as: $u_s^{(ss)} \to v_s^{-1}$, $\Delta^{(ss)} \to v_s^{-2}$, and thus $g^{(ss)} = u_s/\Delta \to v_s$, i.e., a leading order linear increase with (shear) strain rate.

4.6 Steady state pure shear (model 1)

In model 1, only the evolution equation of the isotropic elastic strain has to be modified:

$$\frac{d}{dt}\Delta = 0 = -\lambda_1 T_g \Delta p_g + \alpha_1 u_{ij}^* v_{ij}^*$$

so that inserting Eqs. (71) and (73) yields the isotropic elastic strain in steady state:

$$\Delta_1^{(ss)} = \frac{\alpha_1 v_s^2}{\lambda \lambda_1 (T_g^{(ss)})^2 p_g} = \frac{\Delta^{(ss)}}{p_g} , \qquad (75)$$

for model 1 for constant or Δ-independent p_g.
In some of the numerical implementations, we used $p_g = \Delta - \Delta_\infty$, in order to make Δ relax towards a finite value, with $\Delta_\infty = \log(\rho_\infty/\rho)$, as defined in Eq. (61). This allows to re-write $p_g = \log(\rho_J/\rho_\infty)$, which makes the relaxation term vanish for $\rho_J = \rho_\infty$, negative for larger values and increasingly positive for smaller jamming densities. Unfortunately, it also requires to solve a quadratic equation, resulting in

$$\Delta^{(ss)} = (1/2)\Delta_\infty [1 + \sqrt{1 + 4\Delta^{(ss)}/\Delta_\infty}] ,$$

i.e., an increased steady state elastic strain, representing strain-dilatancy. Note that this approach to achieve finite Δ under steady state shear, increasing with density – as to be expected – is different in philosophy than making the bulk modulus factor B density dependent.
In other of the numerical implementations, we used $p_g = 1 - \Delta_\infty/\Delta$, in order to make Δ relax towards a finite value, resulting in the simpler steady state expression:

$$\Delta_1^{(ss)} = \Delta^{(ss)} - \Delta_\infty = \log(\rho_\infty/\rho_J^{(ss)}) ,$$

with $\Delta_\infty < 0$ for $\rho > \rho_\infty$, which even can change sign dependent on the relative magnitudes of $\Delta^{(ss)}$ and Δ_∞. Note that this approach to achieve finite Δ under steady state shear, increasing with density – as to be expected – is different in philosophy than making the bulk modulus factor B density dependent.

4.7 Discussion of the steady state

Dividing Eq. (73) by (74) yields the deviatoric to elastic strain ratio in steady state (in order to evaluate whether the system is elastically stable or not):

$$g^{(ss)} := \frac{u_s^{(ss)}}{\Delta^{(ss)}} = \frac{\lambda_1 T_g^{(ss)}}{\alpha_1 v_s} , \qquad (76)$$

If the ratio of elastic strains in Eq. (76) is smaller than the elastic stability limit $g^{(ss)} \le g_e = \sqrt{2B/G}$ the system remains in a possibly stable (elastic, jammed) state, while it looses stability if the ratio reaches and/or exceeds the limit value.

Solving numerically the system of equations, including the transient evolution, confirms that the steady state is independent of the density, for model 0, see Sec. 5, as ρ does not appear in the steady state solutions above.

The elastic strain ratio, Eq. (76), which determines whether the system becomes elastically instable in steady state, is not the same as the macroscopic friction at which the material flows plastically. Dividing the steady state shear stress by pressure defines the macroscopic (bulk) "friction": $\mu = \sigma_{ij}^*/P$, which results in the steady state bulk friction:

$$\mu^{(ss)} = \frac{\sigma_{ij}^*}{P} = \frac{\pi_{ij}^{*\,(ss)} + \eta v_{ij}^*}{P_\Delta + P_T} = \frac{\mathcal{G}_\Delta u_{ij}^{(ss)} + \eta v_{ij}^*}{\mathcal{B}_\Delta \Delta^{(ss)} + P_T} . \qquad (77)$$

In the slow strain-rate limit, $\dot\varepsilon_{ij} \to 0$, of Eq. (77), above jamming, $\Delta > 0$, the second terms in nominator and denominator vanish, linearly and quadratically with $T_g \to 0$, respectively, and one has

$$\begin{aligned}\mu_0^{(ss)} &= \frac{\mathcal{G}_\Delta u_s^{(ss)}}{\mathcal{B}_\Delta \Delta^{(ss)}} \\ &= \frac{2(G/B)(\Delta^{(ss)})^{-1} u_s^{(ss)}}{1 + (1/2)(G/B)(u_s^{(ss)})^2 (\Delta^{(ss)})^{-2}} \\ &= \frac{4(G/2B) g^{(ss)}}{1 + (G/2B)(g^{(ss)})^2} = \frac{4 g^{(ss)}}{g_e^2 + (g^{(ss)})^2} . \qquad (78)\end{aligned}$$

For the special case $g^{(ss)} = g_e$, when the elastic limit of stability and the steady state ratio of elastic strains coincide, this translates to: $\mu_0^{(ss)} = 2/g_e$.

4.8 Temperature regularization (model g)

In order to regularize the elastic instability, we introduce a measure for the distance from the elastic limit $g_s = (g - g_e) = (u_s/\Delta - \sqrt{2B/G})$, which can be used to regularize the temperature evolution

$$\frac{d}{dt}T_g = R_T\left[-T_g^2\right] + f_T(\dot\varepsilon_{ij}) + f_g \theta(g_s) g_s , \qquad (79)$$

with the step-function $\theta(g_s > 0) = 1$, and 0 else, so that one has for steady-state pure shear (with model 0):

$$(T_g^{(ss)})^2 = \frac{f_s^2 v_s^2 + f_g \theta(g_s) g_s}{(1 - r^2)} \;, \qquad (80)$$

i.e., just an elevated granular temperature that affects, in turn, the other state-variables (elastic strains) via their respective relaxation terms, as will be shown in the next section 5.

5 Numerical solutions

In order to better understand GSH, we solve the system of equations numerically (with matlab, using ode45) and discuss the features of the simplest GSH type model without any constitutive assumption other than the form of the energy density in Eq. (47), but rather keeping all parameters constant, see table 1.

Units are chosen as $\rho_u = \rho_p = m_p/V_p = 2000\,\mathrm{kg\,m^{-3}}$, with mass, m_p, and volume, V_p, of a single particle, so that the dimensionless density is: $\rho = (\rho_p/\rho_u)\phi = \phi$, while time is measured in units of micro-seconds, $t_u = 1\,\mu$s, and length in units of particle diameters $d_u = d_p = 10^{-4}$m. With these choices, the unit of mass is $m_u = m_p = \rho_p V_p = (\pi/6)\rho_p d_p^3 = (\pi/3)10^{-9}\,$kg, while stress and moduli have units of $\sigma_u = m_u/d_u/t_u^2 = (\pi/3)10^7\,\mathrm{kg\,m^{-1}\,s^{-2}} \approx 10\,$MPa.

The boundary conditions of the numerical solutions are first a preparation by isotropic compression, followed by pure deviatoric (volume-conserving) shear for large strain to approach the critical state, and finally a relaxation without any strain-rate.

5.1 Effect of density and dynamics

Next goal is to understand the behavior of the model at different densities and the effects of the elastic dissipation parameter T_e and the temperature regularization f_g.

The initial preparation starts from an un-jammed state at $\rho(0) = 0.58$, and is applied up to different target densities $\rho = 0.61, 0.62, 0.63, 0.68, 0.74$, and 0.80 during $t_p = 1000$. From this point on, pure shear is applied for $t_s = 5000$ and the final relaxation is applied for $t_r = 4000$.

First, the effect of T_e on the system is studied in Figs. 7 and 8. In order to understand the behavior, shear stress is plotted against pressure and the ratio of the deviatoric-to-isotropic elastic strains is plotted against time. In the former Fig. 7, T_e is practically zero and has no effect at all, whereas in the latter Fig. 8, the finite T_e causes a reduced T_g in steady state, as well as a much more rapid (exponential) relaxation to the static state (shorter magenta lines). Due the decreased T_g, the other state variables Δ and u_s are increased, whereas their ratio is also decreased, see Eq. (76).

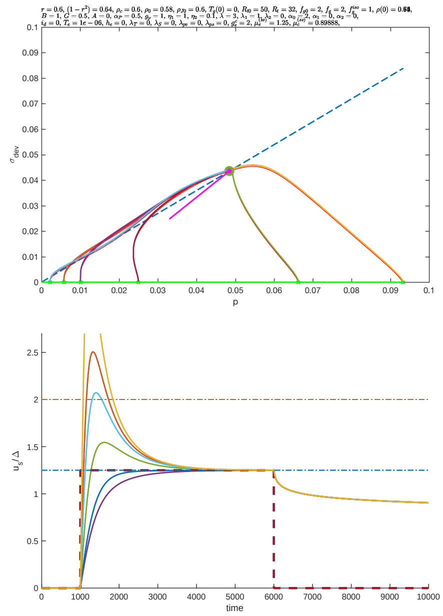

Fig. 7 Case A (model 0): Shear stress plotted against pressure (top) and deviatoric-to-isotropic elastic strain ratio plotted against time (bottom). The green lines (on the horizontal) represent the isotropic preparation, the magenta lines (overlapping), the final relaxation, with the big solid dots as theoretically predicted steady state $\sigma_{\rm dev} = \mu_0^{(ss)} p$. The dashed horizontal lines represent g_e (upper) and $g^{(ss)}$ (lower), for $T_e = 10^{-6}$.

The effect of the new temperature production term with $f_g = 4.10^{-4}$ is then tested in Fig. 9, with otherwise the same settings as in case B. Only those cases that overshoot g_e are affected. One of them, the lowermost density case, is completely destabilized by the increase in T_g, while the other (second lowest density) remains above, but moves closer to g_e and remains there for some longer time. This proofs that the production of T_g due to the elastic instability allows to regularize the systems' behavior by dynamic means, i.e., by generation of more T_g keeps the system closer to the elastic instability. However, if too much T_g is produced, this destabilizes the system and allows it to explore the plastic, collisional steady state with very large T_g and – at the same time – small u_s and Δ.

Finally, we study the effect of different f_g on a system at low density $\rho = 0.62$ using model 1 (case E) in Fig. 10, plotting again shear against normal stress in

	m.	T_e	f_g	B	G	λ	λ_1	α_1	R_{T0}	r	R_T	f_s	f_v	η_s	χ	g_e	$g^{(ss)}$	μ_0
A	0	10^{-6}	0	1	0.5	3	1	2	50	0.6	32	2	1	1	0.1	2	1.250	0.90
B	0e	2.10^{-4}	0	1	0.5	3	1	2	50	0.6	32	2	1	1	0.1	2	1.165	0.87
C	0eg	2.10^{-4}	4.10^{-4}	1	0.5	3	1	2	50	0.6	32	2	1	1	0.1	2	1.165	0.87
D1	0	0	0	1	0.5	3	1	...	50	0.6	32	2	1	0.1	0.1	2	...	1
D2	0g	0	5.10^{-5}	1	0.5	3	1	...	50	0.6	32	2	1	0.1	0.1	2	...	1
D3	0eg	2.10^{-4}	5.10^{-5}	1	0.5	3	1	...	50	0.6	32	2	1	0.1	0.1	2	...	1
E	1eg	2.10^{-4}	...	1	0.5	10	5	2	50	0.6	32	2	1	0.1	0.1	2	...	1

Table 1 Summary of parameters used for the numerical solutions of GSH, where m. indicates the model used and dots replace values that are varied in this case.

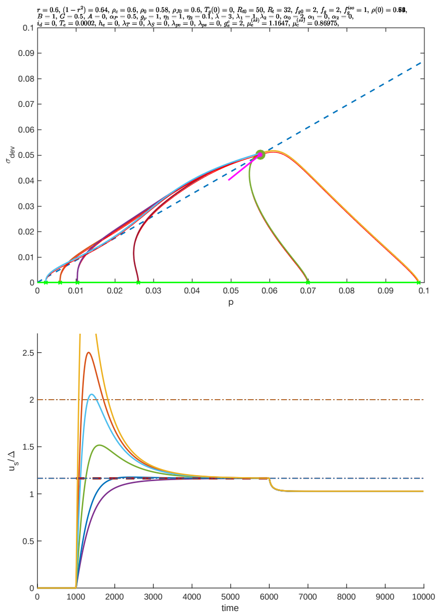

Fig. 8 Case B (model 0e with $T_e = 2.10^{-4}$): Shear stress plotted against pressure (top) and deviatoric-to-isotropic elastic strain ratio plotted against time (bottom). The green lines (on the horizontal) represent the isotropic preparation, the magenta lines (overlapping), the final relaxation, with the big solid dots as theoretically predicted steady state $\sigma_{\text{dev}} = \mu_0^{(ss)} p$. The dashed-dotted horizontal lines represent g_e (upper) and $g^{(ss)}$ (lower), for finite T_e, while the dashed lines correspond to the critical state limits.

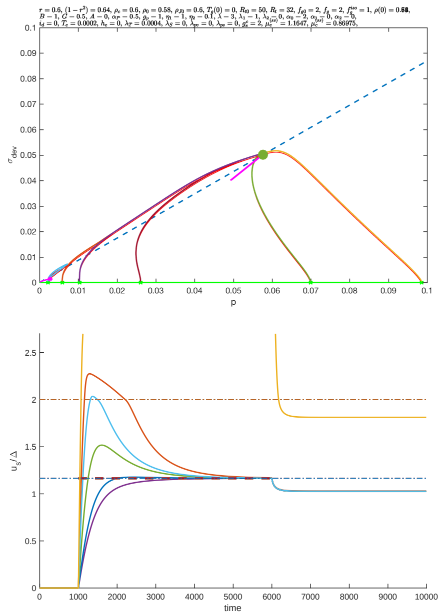

Fig. 9 Case C (model 0eg with $T_e = 2.10^{-4}$ and $f_g = 4.10^{-4}$): Shear stress plotted against pressure (top) and deviatoric-to-isotropic elastic strain ratio plotted against time (bottom). The green lines (on the horizontal) represent the isotropic preparation, the magenta lines (overlapping), the final relaxation, with the big solid dots as theoretically predicted steady state $\sigma_{\text{dev}} = \mu_0^{(ss)} p$. The dashed-dotted horizontal lines represent g_e (upper) and $g^{(ss)}$ (lower), while the dashed lines correspond to the critical state limits.

the upper panel and elastic shear to normal strain in the lower.

The data are complemented by two more simulations, one with model 0, using the same density, and one with the same model 1 (with $f_g = 0$), but compressed up to density $\rho = 0.64$. The former is behaving very different, reaching the highest steady state level of u_s/Δ in steady state and also relaxing to a large value, $g > g_e$, because $f_g = 0$. The compression to higher density shows that this system, in steady state, is not reaching the elastic stability limit (upper diagonal) and, at the end of shear, is just relaxing deeper into the elastic cone (magenta line).

From the lower plot it is clear that all data reach their respective steady state and relax after shear is stopped. The four simulations with model 1 correspond to the four in-between curves, where the largest value of f_g provides the curve that is closest to g_e, i.e., the temperature regularization succeeds to keep the system very close to the elastic stability limit, just by adding considerable temperature.

From the upper panel, we further learn that the model g does not affect the system much if f_g is close to zero, but that the increased level of T_g, created by the increasing f_g values, keeps the system very close to the stability limit (yellow curve) and allows the system to relax to much smaller values stress, closely embracing the cricial state line μ_0. In contrast to model 0, the modified model 1 with large enough f_g thus reaches a very much relaxed final state, at rather small values of stress, within the elastic stability cone.

This system thus has yielded when reaching the elastic limit, g_e, there the temperature production kicks in, proportional to f_g, and keeps the system close to g_e, but pushing it towards the plastic equilibrium $\pi = 0$. In the steady state the system is not reaching its desired equilbrium, and also during relaxation it is not just getting there, but rather jamming and becoming elastic again.

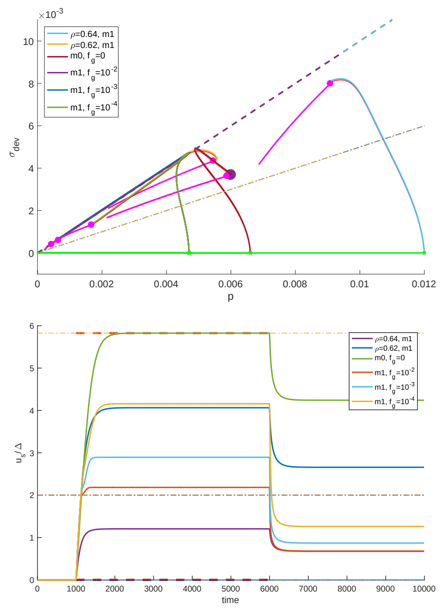

Fig. 10 Case E (model 1) with $T_e = 2.10^{-4}$ and different $f_g = 0$, 10^{-4}, 10^{-3}, and 10^{-2}: Shear stress plotted against pressure (top) and deviatoric-to-isotropic elastic strain ratio plotted against time (bottom). The single simulation with model 0 corresponds to the uppermost curve in the lower panel and the big solid dot is its theoretically predicted steady state. The single simulation compressed towards larger density is the lowermost curve in the lower panel, and the rightmost curve in the upper panel. There, the green lines (on the horizontal) represent the isotropic preparation, while the magenta lines show the final relaxation after shear stops. The slopes in the upper panel represent $\mu_0 = 2/g_e = 1$ and $\mu = 0.5$ (to guide the eye), while the dashed-dotted horizontal lines in the lower panel represent g_e (lower) and $g^{(ss)}$ (upper, for model 0).

5.2 Effect of dilatancy and dynamics

Next goal is to understand the behavior of the model at constant density, with different dilatancy parameters, α_1, and the effects of the elastic dissipation parameter T_e and the temperature regularization f_g.

The initial preparation starts from an un-jammed state at $\rho(0) = 0.58$, and is applied up to target density $\rho = 0.65$, during $t_p = 1000$. From this point on, pure shear is applied for $t_s = 5000$ and the final relaxation is applied for $t_r = 4000$, like before.

The values of α_1 are chosen such that a few of the data remain within the elastic instability limit $u_s/\Delta < g_e$, but a few overshoot, as can be seen in the lower panels of Figs. 11, 12, and 13.

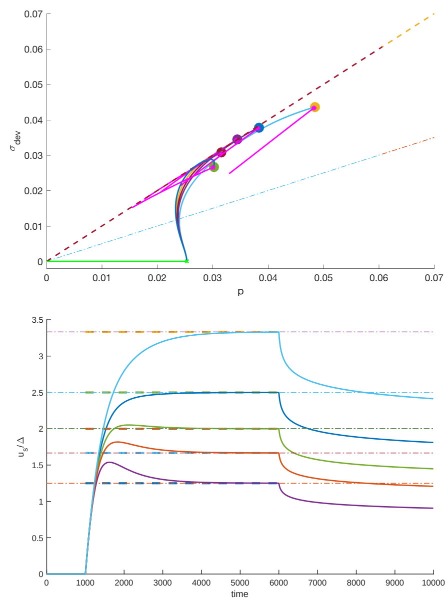

Fig. 11 Case D1 (model 0): Shear stress plotted against pressure (top) and deviatoric-to-isotropic elastic strain ratio plotted against time (bottom), for the same density, $\rho = 0.65$, and different values of $\alpha_1 = 0.75$, 1, 1.25, 1.5, 2 (from top to bottom). The green lines (on the horizontal) represent the isotropic preparation, the curves the evolution during pure shear up to the dots, representing the steady state solution, $\sigma_{\mathrm{dev}} = \mu_0^{(ss)} P$, see Eq. (78) while the magenta lines show the final relaxation, with $T_e = 0$. The slopes in the top panel correspond to $\mu_0^{(ss)} = 1$ and $\mu_c = 0.5$, to guide the eye, and the dashed horizontal lines in the lower panel represent the analytical values $g_e = 2$ and various $g^{(ss)}$, see Eq. (76).

First, the effect of f_g on the system is studied in Figs. 11, 12, and later the effect of T_e in Fig. 13. Again, shear stress is plotted against pressure and the ratio of the deviatoric-to-isotropic elastic strains is plotted

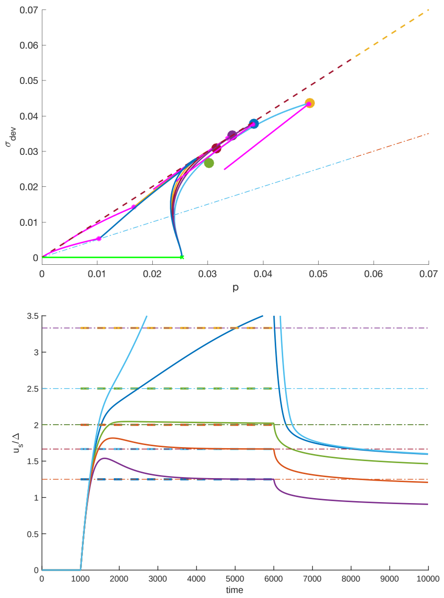

Fig. 12 Case D2 (model 0): with $T_e = 0$ and $f_g = 5.10^{-5}$. All parameters are the same as in Fig. 11, except for $f_g = 5.10^{-5}$, which causes the steady state granular temperature in Eq. (80) - not shown explicitly - which causes the different behavior of the upper curves.

against time. In the former, Fig. 11, T_e and f_g are practically zero and have no effect at all, but an increasing dilatancy parameter, α_1 causes the system into decreasing levels of $g = u_s/\Delta$ during shear. The two lowermost curves remain within the elastic instability limit, the intermediate value $\alpha_1 = 1.25$ displays a slight overshoot but hits $g_e = 2$ in the steady state, while the upper two curves are clearly beyond the elastically stable regime $g > g_e$. In the shear stress to normal stress plot, the different α_1 values lead to different steady states (thick dots) and a slow relaxation (magenta lines).

When temperature regularization is active in Fig. 12, the curves in the stable regime are not affected, the intermediate case is slightly modified and the upper two curves (smaller two α_1) are, again, considerably affected by the generation of T_g, i.e., the much larger T_g causes both elastic strains to relax towards the plastic limit – see the curves in the lower left plot of the shear to normal stress plot.

In the last Fig. 13, the finite T_e causes a reduced T_g in steady state, which results also in smaller $u_s^{(ss)}/\Delta$, see Eq. (76). During final relaxation, T_e is also causing a much more rapid (exponential) relaxation to the static state (shorter magenta lines).

Note that T_e has an effect within and outside, whereas f_g is only active outside the elastically stable regime.

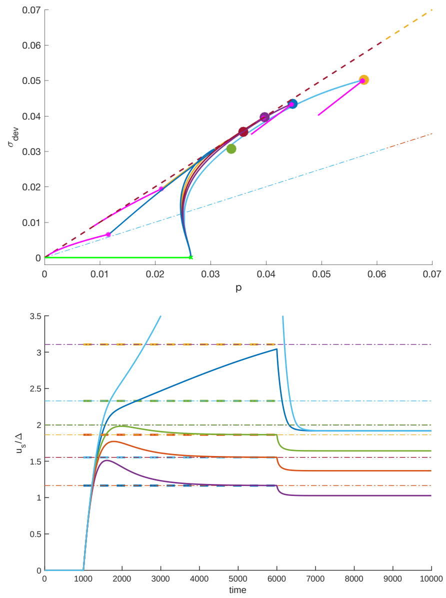

Fig. 13 Case D3 (model 0): with $T_e = 2.10^{-4}$ and $f_g = 5.10^{-5}$. All other parameters are the same as in Fig. 11, except for $f_g = 5.10^{-5}$, which causes the steady state granular temperature in Eq. (80) - not shown explicitly - which causes the different behavior of the upper curves.

6 Conclusion and Outlook

The focus of this paper was on yielding and unjamming/jamming of granular matter, which was inspired by the late Bob Behringer, to whom this work is dedicated. In an attempt to combine theoretical considerations with numerical/experimental observations on granular matter, the authors propose a minimalist macroscopic model to capture qualitatively all states of granular matter, and which even can be solved analytically in several special, limit cases.

The system considered was a representative volume element of granular matter, without gradients and no walls. The granular material was considered in fluid-like and solid-like states, as well as during continuous changes across the states as well as during and after the transition from elastically stable to instable, which is the novel contribution, since the latter states can be highly dynamic – something that is not possible, e.g., in standard elasto-plastic approaches or critical state theory.

Based on the rather complex, but versatile granular solid hydrodynamics (GSH), a much simplified qualitative model that includes un-jammed, fluid-like states as well as jammed solid-like states (elastically stable) was proposed and studied – analytically as well as numerically. Furthermore, various transitions and intermediate states could be identified and better understood in the framework of the simplemost GSH type model, which has only three state-variables, density, elastic strain (isotropic and deviatoric) and granular temperature, unifying all the states of granular matter we could imagine. In order to keep this universal modeling attempts transparent, the model equations were much simplified by making most parameters constant, so that the structure of the model equations rather than the constitutive assumptions could be tested.

This over-simplified model – even though not quantitatively calibrated, neither with experiments nor with particle simulations – nevertheless, is capable of following the granular system from very low (dilute granular gas) to very high densities (dense jammed granular solid), including various transients and transitions. Furthermore, the model was generalized to include soft particle phenomenology, as inspired by recent soft particle simulations, as well as a strictly non-thermal limit (removing the granular temperature), as well as perfectly plastic, elastic or intermediate states – involving a critical state and an elastic instability, which was actually the main focus and reason to start this research.

The *first mode of isotropic un-jamming* appears trivial; decompression of the system makes the density decrease and un-jamming takes place when the elastic strain vanishes. However, the density at which un-jamming takes place depends on the history of the packing. Perturbations by tapping or over-compression both can result in (un-)jamming densities considerably larger than the lowest possible one, the random loose packing density. The longer/stronger the system is perturbed, the larger the jamming density will be, but the approach to this upper limit is realized very slowly. *Whether there are well defined random loose and random close packing densities, below/above which the system cannot jam/un-jam anymore – or if not – is an important open question: both limit densities are very sensible to the protocol one uses to approach and realize/measure them.*

The *second mode of un-jamming is by plastic yielding*, which involves irreversible deformations/restructuring of the solid granular matter, but does not involve dynamics or granular temperature – at least not in the classical picture. Plastic events occur with a certain probability, see Ref. [53], which is larger the closer the system is to un-jamming or the larger the elastic shear strain (stress) is which was previously accumulated. This mode involves the more classical world of elasto-plastic continuum mechanics and rheology for example see Refs. [119,40,60]. The evident lack of a dynamic state variable is at the origin of many difficulties with those elasto-plastic concepts, in particular when the deformation rates become larger and larger. Modern concepts like fluidity or non-local models have been proposed during the last years to overcome this problem [119,120,41,43].

The *third mode of un-jamming is a transition* occuring via an elastic instability, i.e., the loss of convexity, and then involves deformations of the solid granular matter that can occur without penalty, at the onset of concavity (elastic instability) or, are even activated/pushed by the external stresses (in the concave regime). This mode is different from plastic yielding, since it allows for dynamics (granular temperature) to build up, grow, and eventually push back the system into a mechanically stable elastic state before/while it is dissipated. How much different – if at all – plastic and elastic yielding really are has to be seen, and is subject of current ongoing research.

Outlook: Many remaining challenges, besides the quantitative calibration of the universal model for granular matter, involve the understanding of all the different mechanisms of relaxation, creation and destruction of energy in the elastic strain degrees of freedom as well as the dynamic, kinetic, granular ones. Related open questions are: What is the relaxation/evolution dynamics of the state-variables below, above and during un-jamming/jamming? What are the differences and similarities of the driving forces/mechanisms? And, can they all be combined in a single universal model as attempted in this study?

Acknowledgements We thank Sampan Arora for many GSH discussions and the first version of the simple GSH-solver, as well as Anthony Thornton, Thomas Weinhart, and Itai Einav for valuable discussions about GSH.

References

1. J. T. Jenkins and S. B. Savage. A theory for the rapid flow of indentical, smooth, nearly elastic, spherical particles. *J. Fluid Mech.*, 130:187–202, 1983.
2. H. Di Benedetto and F. Darve. Comparison of rheological laws in rotational kinematics. *Journal de Mecanique Theorique et Appliquee*, 2(5):769, 1983.
3. J. P. Hansen and I. R. McDonald. *Theory of Simple Liquids*. Academic Press, 1986.
4. F. Darve, E. Flavigny, and M. Meghachou. Yield surfaces and principle of superposition: revisit through in-

crementally non-linear constitutive relations. *International Journal of Plasticity*, 11(8):927–945, 1995.
5. H. M. Jaeger, S. R. Nagel, and R. P. Behringer. The physics of granular materials. *Physics Today*, 49(4):32–38, 1996.
6. Heinrich M. Jaeger, Sidney R. Nagel, and Robert P. Behringer. Granular solids, liquids, and gases. *Rev. Mod. Phys.*, 68(4):1259–1273, 1996.
7. B. Miller, C. O'Hern, and R. P. Behringer. Stress Fluctuations for Continously Sheared Granular Materials. *Phys. Rev. Lett.*, 77:3110–3113, 1996.
8. C. T. Veje, D. W. Howell, R. P. Behringer, S. Schöllmann, S. Luding, and H. J. Herrmann. Fluctuations and flow for granular shearing. In H. J. Herrmann, J. P. Hovi, and S. Luding, editors, *Physics of dry granular media - NATO ASI Series E 350*, page 237, Dordrecht, 1998. Kluwer Academic Publishers.
9. Pieter A. Vermeer. *Continuous and discontinuous modelling of cohesive-frictional materials*, volume 568. Springer Science & Business Media, 2001.
10. Thorsten Pöschel and Stefan Luding. *Granular gases*, volume 564. Springer Science & Business Media, 2001.
11. J. Geng, D. Howell, E. Longhi, R. P. Behringer, G. Reydellet, L. Vanel, E. Clément, and S. Luding. Footprints in sand : The response of a granular material to local perturbations. *Phys. Rev. Lett.*, 87, 2001.
12. C. S. O'Hern, Langer, and S. R. Nagel. Force distributions near jamming and glass transitions. *Phys. Rev. Lett.*., 86:111–114, 2001.
13. S. D. C. Walsh and A. Tordesillas. A thermomechanical approach to the development of micropolar constitutive models of granular media. *Acta mechanica*, 167(3):145–169, 2004.
14. K. E. Daniels and R. P. Behringer. Hysteresis and Competition between Disorder and Crystallization in Sheared and Vibrated Granular Flow. *Phys. Rev. Lett.*, 94(6):168001, 2005.
15. K. E. Daniels and R. P. Behringer. Characterization of a freezing/melting transition in a vibrated and sheared granular medium. *J. Stat. Mech. – Theory and Experiment*, 2006, 2006.
16. R. P. Behringer, Karen E. Daniels, Trushant S. Majmudar, and Matthias Sperl. Fluctuations, correlations and transitions in granular materials: statistical mechanics for a non-conventional system. *Philosophical Transactions of the Royal Society A: Mathematical, Physical and Engineering Sciences*, 366(1865), 2008.
17. M. Lätzel, S. Luding, H. J. Herrmann, D. W. Howell, and R. P. Behringer. Comparing simulation and experiment of a 2D granular Couette shear device. *Eur. Phys. J. E*, 11(4):325–333, 2003.
18. Itai Einav and Alexander M. Puzrin. Pressure-dependent elasticity and energy conservation in elastoplastic models for soils. *Journal of Geotechnical and Geoenvironmental Engineering*, 130(1):81–92, 2004.
19. Corey S. O'Hern, Andrea J. Liu, and Sidney R. Nagel. Effective temperatures in driven systems: static versus time-dependent relations. *Phys. Rev. Lett.*, 93(16), 2004.
20. Stefan Luding. Granular media: Information propagation. *Nature*, 435(7039):159–160, 2005.
21. Ning Xu, Corey S. O'Hern, and Lou Kondic. Stabilization of nonlinear velocity profiles in athermal systems undergoing planar shear flow. *Phys. Rev. E*, 72(4):041504+, 2005.
22. F. Alonso-Marroquin, S. Luding, H. J. Herrmann, and I. Vardoulakis. Role of anisotropy in the elastoplastic response of a polygonal packing. *Phys. Rev. E*, 71(5), 2005.
23. J. T. Jenkins. Dense shearing flows of inelastic discs. *Physics of fluids*, 18(10):103307, 2006.
24. N. Xu and C. S. O'Hern. Measurements of the yield stress in frictionless granular systems. *Phys. Rev. E*, 73:61303, 2006.
25. Jasna Brujić, Chaoming Song, Ping Wang, Christopher Briscoe, Guillaume Marty, and Hernán A. Makse. Measuring the Coordination Number and Entropy of a 3D Jammed Emulsion Packing by Confocal Microscopy. *Phys. Rev. Lett.*, 98(24):248001, 2007.
26. L. Sibille, F. Nicot, F. V. Donze, and F. Darve. Material instability in granular assemblies from fundamentally different models. *Int. J. Numer. Anal. Meth. Geomech.*, 31:457–481, 2007.
27. Silke Henkes, Corey S. O'Hern, and Bulbul Chakraborty. Entropy and temperature of a static granular assembly: an ab initio approach. *Phys. Rev. Lett.*, 99(3):038002, 2007.
28. T. S. Majmudar, M. Sperl, S. Luding, and R. P. Behringer. Jamming Transition in Granular Systems. *Phys. Rev. Lett.*, 98(5):058001+, 2007.
29. R. P. Behringer, Dapeng Bi, B. Chakraborty, S. Henkes, and R. R. Hartley. Why do granular materials stiffen with shear rate? Test of novel stress-based statistics. *Phys. Rev. Lett.*, 101(26), 2008.
30. Dapeng Bi and Bulbul Chakraborty. Rheology of granular materials: dynamics in a stress landscape. *Philosophical Transactions of the Royal Society of London A: Mathematical, Physical and Engineering Sciences*, 367(1909):5073–5090, 2009.
31. Silke Henkes and Bulbul Chakraborty. Statistical mechanics framework for static granular matter. *Phys. Rev. E*, 79:61301, 2009.
32. Luc Sibille, Francois Nicot, and Félix Darve. Analysis of failure occurrence from direct simulations. *European Journal of Environmental and Civil Engineering*, 13(2):187–201, 2009.
33. Richard Wan and Nicot, Francois. Micromechanical Formulation of Stress Dilatancy as a Flow Rule in Plasticity of Granular Materials. *Journal of Engineering Mechanics*, 136(5):589–598, 2010.
34. J. T. Jenkins and D. Berzi. Dense inclined flows of inelastic spheres: tests of an extension of kinetic theory. *Granul. Matter.*, 12, 2010.
35. F. Nicot, A. Daouadji, F. Laouafa, and F. Darve. Second-order work, kinetic energy and diffuse failure in granular materials. *Granular Matter*, 13:19, 2011.
36. R. G. Wan, M. Pinheiro, and P. J. Guo. Elastoplastic modelling of diffuse instability response of geomaterials. *Int. J. Numer. Anal. Meth. Geomech.*, 35(2):140–160, 2011.
37. Stefan Luding and Fernando Alonso-Marroqu'in. The critical-state yield stress (termination locus) of adhesive powders from a single numerical experiment. *Granul. Matter.*, 13:109–119, 2011.
38. S. Luding and E. S. Perdahcioglu. A Local Constitutive Model with Anisotropy for Various Homogeneous 2D Biaxial Deformation Modes. *Chemie Ingenieur Technik*, 83(5):672–688, 2011.
39. D. Bi, J. Zhang, B. Chakraborty, and R. P. Behringer. Jamming by shear. *Nature*, 480(7377):355–358, 2011.
40. Itai Einav. The unification of hypo-plastic and elastoplastic theories. *International Journal of Solids and Structures*, 49(11-12):1305–1315, 2012.

41. J. Zhao and N. Guo. Unique critical state characteristics in granular media considering fabric anisotropy. *Géotechnique*, 63(8):695–704, 2013.
42. Jie Ren, Joshua A. Dijksman, and Robert P. Behringer. Reynolds Pressure and Relaxation in a Sheared Granular System. *Phys. Rev. Lett.*, 110:18302, 2013.
43. D. L. Henann and K. Kamrin. A predictive, size-dependent continuum model for dense granular flows. *Proceedings of the National Academy of Sciences*, 110(17):6730–6735, 2013.
44. Somayeh Farhadi and Robert P. Behringer. Dynamics of sheared ellipses and circular disks: effects of particle shape. *Phys. Rev. Lett.*, 112(14):148301, 2014.
45. N. P. Kruyt, O. Millet, and F. Nicot. Macroscopic strains in granular materials accounting for grain rotations. *Granul. Matter.*, pages 1–12, 2014.
46. David M. Walker, Antoinette Tordesillas, Jie Ren, Joshua A. Dijksman, and Robert P. Behringer. Uncovering temporal transitions and self-organization during slow aging of dense granular media in the absence of shear bands. *Europhys. Lett.*, 107(1):18005, 2014.
47. N. Kumar, S. Luding, and V. Magnanimo. Incremental stress and microstructural response of granular soils under undrained axisymmetric deformation. In Kenichi Soga, Krishna Kumar, Giovanna Biscontin, and Matthew Kuo, editors, *Geomechanics from Micro to Macro*, pages 115–121, Reggio Calabria (Italy), 14-18 September 2009, 2014. CRC Press/Balkema.
48. Romain Mari, Ryohei Seto, Jeffrey F. Morris, and Morton M. Denn. Discontinuous shear thickening in brownian suspensions by dynamic simulation. *Proceedings of the National Academy of Sciences*, 112(50):15326–15330, 2015.
49. Nicolas Brodu, Joshua A. Dijksman, and Robert P. Behringer. Spanning the scales of granular materials through microscopic force imaging. *Nature communications*, 6:6361+, 2015.
50. N. Berger, E. Azema, J.-F. Douce, and F. Radjai. Scaling behaviour of cohesive granular flows. *Europ. Phys. Lett.*, 112:64004, 2015.
51. N. Hadda, L. Sibille, F. Nicot, and F. Darve. Failure in granular media from an energy viewpoint. *Granular Matter*, 18:50, 2016.
52. Stefan Luding. Granular matter: So much for the jamming point. *Nature*, 12(6):531–532, June 2016.
53. Nishant Kumar and Stefan Luding. Memory of jamming–multiscale models for soft and granular matter. *Granular matter*, 18(3):1–21, 2016.
54. Sudeshna Roy, Stefan Luding, and Thomas Weinhart. A general(ized) local rheology for wet granular materials. *New Journal of Physics*, 19:043014, 2017.
55. Itai Einav and Mario Liu. Hydrodynamic derivation of the work input to fully and partially saturated soils. *Journal of the Mechanics and Physics of Solids*, 110:205–217, 2018.
56. S. Athani and P. Rognon. Mobility in granular materials upon cyclic loading. *Granular Matter*, 20:67, 2019.
57. D. Vescovi, D. Berzi, and C. di Prisco. Fluid–solid transition in unsteady, homogeneous, granular shear flows. *Granular Matter*, 20:27, 2019.
58. Antoine Wautier, Stéphane Bonelli, and Francois Nicot. Micro-inertia origin of instabilities in granular materials. *International Journal for Numerical and Analytical Methods in Geomechanics*, 42(9):1037–1056, 2018.
59. Julia Boschan, Stefan Luding, and Brian Tighe. Jamming and irreversibility. *Granular Matter*, 2019.
60. Alexandre Nicolas, Ezequiel E. Ferrero, Kirsten Martens, and Jean-Louis Barrat. Deformation and flow of amorphous solids: An updated review of mesoscale elastoplastic models. *Rev. Mod. Phys.*, 90(4):045006, 2018.
61. Bernard Cambou, Felix Darve, and Francois Nicot. Particle methods in geomechanics. *International Journal for Numerical and Analytical Methods in Geomechanics*, 43:831–832, 04 2019.
62. E. Ando, J. Dijkstra, E. Roubin, C. Dano, and E. Boller. A peek into the origin of creep in sand. *Granular Matter*, 21:11, 2019.
63. M. R. Kuhn and A. Daouadij. Stress fluctuations during monotonic loading of dense three-dimensional granular materials. *Granular Matter*, 21:10, 2019.
64. M. M. Bandi, Prasenjit Das, Oleg Gendelman, H. George, E. Hentschel, and Itamar Procaccia. Universal scaling laws for shear induced dilation in frictional granular media. *Granular Matter*, 21:40, 2019.
65. Aaron S. Baumgarten and Ken Kamrin. A general fluid–sediment mixture model and constitutive theory validated in many flow regimes. *Journal of Fluid Mechanics*, 861:721–764, 2019.
66. Yimin Jiang and Mario Liu. Granular elasticity without the coulomb condition. *Physical review letters*, 91(14):144301, 2003.
67. Yimin Jiang and Mario Liu. Energetic instability unjams sand and suspension. *Physical review letters*, 93(14):148001, 2004.
68. Yimin Jiang and Mario Liu. From elasticity to hypoplasticity: dynamics of granular solids. *Physical review letters*, 99(10):105501, 2007.
69. Yimin Jiang and Mario Liu. Granular solid hydrodynamics. *Granular Matter*, 11(3):139, 2009.
70. Yimin Jiang and Mario Liu. Applying GSH to a wide range of experiments in granular media. *The European Physical Journal E*, 38(3):15, 2015.
71. Yimin Jiang and Mario Liu. Why granular media are thermal, and quite normal, after all. *The European Physical Journal E*, 40(1):10, 2017.
72. L. D. Landau and E. M. Lifshitz. *Fluid Mechanics*. Butterworth-Heinemann, 1987.
73. S. Luding. Towards dense, realistic granular media in 2D. *Nonlinearity*, 22(12):R101–R146, 2009.
74. Ramón Garcia-Rojo, Stefan Luding, and Javier J. Brey. Transport coefficients for dense hard-disk systems. *Physical review. E, Statistical, nonlinear, and soft matter physics*, 74(6 Pt 1), 2006.
75. Dalila Vescovi and Stefan Luding. Merging fluid and solid granular behavior. *Soft matter*, 12(41):8616–8628, 2016.
76. L. D. Landau and E. M. Lifshitz. *Theory of Elasticity*. Butterworth-Heinemann, 1986.
77. R. M. Nedderman. *Statics and kinematics of granular materials*. Cambr. Univ. Press, Cambridge, 1992.
78. Joe D. Goddard. Continuum modeling of granular media. *Applied Mechanics Reviews*, 66(5):050801, 2014.
79. Mario Liu. Thermodynamics and constitutive modeling. In Itai Einav & Eleni Gerolymatou, editor, *ALERT Doctoral School 2018: Energetical Methods in Geomechanics / Chapter 2: Thermodynamics and Constitutive Modeling*, `http://alertgeomaterials.eu/data/school/2018/2018_ALERT_school.pdf`, 2018.
80. D. Krijgsman and S. Luding. 2D cyclic pure shear of granular materials, simulations and model. In S. Luding and A. Yu, editors, *Powders Grains 2013*, pages 1226–1229, Sydney, Australia, 2013. Balkema.

81. N. Kumar, S. Luding, and V. Magnanimo. Macroscopic model with anisotropy based on micro–macro information. *Acta Mechanica*, 225(8):2319–2343, 2014.
82. D. Krijgsman and S. Luding. Simulating granular materials by energy minimization. *Comp. Part. Mech.*, 3(4):463–475, 2016.
83. J. Zhang, T. Majmudar, A. Tordesillas, and R. Behringer. Statistical properties of a 2D granular material subjected to cyclic shear. *Granul. Matter.*, 12(2):159–172, 2010.
84. Karin A. Dahmen, Yehuda Ben-Zion, and Jonathan T. Uhl. Micromechanical Model for Deformation in Solids with Universal Predictions for Stress-Strain Curves and Slip Avalanches. *Phys. Rev. Lett.*, 102:175501, 2009.
85. Dong Wang, Jie Ren, Joshua A. Dijksman, Hu Zheng, and Robert P. Behringer. Microscopic origins of shear jamming for 2d frictional grains. *Phys. Rev. Lett.*, 120(20):208004, 2019.
86. J. Bardeen. Critical fields and currents in superconductors. *Rev Mod Phys 34.667*, 34(4), 1962.
87. C. Liu and S. R. Nagel. Sound in a granular material: Disorder and nonlinearity. *Phys. Rev. B*, 48:15646, 1993.
88. A. S. J. Suiker, R. de Borst, and C. S. Chang. Micromechanical modelling of granular material. Part 1: Derivation of a second-gradient micro-polar constitutive theory. *Acta Mechanica*, 149(1), 2001.
89. E. Somfai, J. N. Roux, J. H. Snoeijer, M. van Hecke, and W. van Saarloos. Elastic wave propagation in confined granular systems. *Phys. Rev. E*, 72:21301, 2005.
90. B. P. Tighe and J. E. S. Socolar. Nonlinear elastic stress response in granular packings. *Phys. Rev. E*, 77(3):031303+, 2007.
91. X. Jia. Codalike multiple scattering of elastic waves in dense granular media. *Phys. Rev. Lett.*, 93(15):154303, Oct 2004.
92. Michael Mayer and Mario Liu. Propagation of elastic waves in granular solid hydrodynamics. *Physical Review E*, 82(4):042301, 2010.
93. A. Merkel and S. Luding. Enhanced micropolar model for wave propagation in ordered granular materials. *Int. J. of Solids and Structures*, 106-107:i91–105, 2017.
94. N. P. Kruyt. Three-dimensional lattice-based dispersion relations for granular materials. In J. Goddard, P. Giovine, and J. T. Jenkins, editors, *IUTAM-ISIMM Symposium on Mathematical Modeling and Physical Instances of Granular Flows*, pages 405–415, Reggio Calabria (Italy), 14-18 September 2009, 2010. AIP.
95. Rohit Kumar Shrivastava and Stefan Luding. Effect of disorder on bulk sound wave speed: a multiscale spectral analysis. *Nonlin. Processes Geophys.*, 24:435–454, 2017.
96. C. E. Maloney and A. Lematextasciicircumitre. Amorphous systems in athermal, quasistatic shear. *Phys. Rev. E*, 74:16118, 2006.
97. A. J. Liu and S. R. Nagel. Nonlinear dynamics: Jamming is not just cool any more. *Nature*, 396(6706):21–22, 1998.
98. Paul C. Martin, O. Parodi, and Peter S. Pershan. Unified hydrodynamic theory for crystals, liquid crystals, and normal fluids. *Physical Review A*, 6(6):2401, 1972.
99. H. B. Callen. *Thermodynamics and an introduction to thermostatistics.* John Wiley & Sons, 1985.
100. Peter Kostädt and Mario Liu. Three ignored densities, frame-independent thermodynamics, and broken Galilean symmetry. *Physical Review E*, 58(5):5535, 1998.
101. Oliver Müller, Mario Liu, Harald Pleiner, and Helmut R. Brand. Transient elasticity and polymeric fluids: Small-amplitude deformations. *Physical Review E*, 93(2):023113, 2016.
102. Oliver Müller, Mario Liu, Harald Pleiner, and Helmut R. Brand. Transient elasticity and the rheology of polymeric fluids with large amplitude deformations. *Physical Review E*, 93(2):023114, 2016.
103. Alan A. Long, Dmitry V. Denisov, Peter Schall, Todd C. Hufnagel, Xiaojun Gu, Wendelin J. Wright, and Karin A. Dahmen. From critical behavior to catastrophic runaways: comparing sheared granular materials with bulk metallic glasses. *Granular Matter*, 2019.
104. K. Saitoh, V. Magnanimo, and S. Luding. Master equation for the probability distribution functions of overlaps between particles in two dimensional granular packings. *arXiv:1311.5359*, 2014.
105. Kuniyasu Saitoh, Norihiro Oyama, Fumiko Ogushi, and Stefan Luding. Transition rates for slip-avalanches in soft athermal disks under quasi-static simple shear deformations. *Soft Matter*, 15:3487–3492, 2019.
106. D. Kolymbas. *Introduction to Hypoplasticity.* Balkema, Rotterdam, 2000.
107. Yimin Jiang and Mario Liu. Proportional paths, barodesy, and granular solid hydrodynamics. *Granular Matter*, 15(2):237–249, 2013.
108. D.P. Bi, J. Chang, B. Chakraborty, and R.P. Behringer. *Nature, 480, 355*, 2011.
109. Somayeh Farhadi and Robert P. Behringer. *Phys. Rev. Lett. 112, 148301*, 2014.
110. Y. Jiang and M. Liu. A brief review of granular elasticity. *The European Physical Journal E - Soft Matter*, 22(3):255, 2007.
111. Y. Jiang and M. Liu. Incremental stress-strain relation from granular elasticity: Comparison to experiments. *Phys. Rev. E (Statistical, Nonlinear, and Soft Matter Physics)*, 77(2):021306, 2008.
112. M. Mayer and M. Liu. Propagation of elastic waves in granular solid hydrodynamics. *Phys. Rev. E*, 82:042301, 2010.
113. B.O. Hardin and F.E. Richart. Elastic wave velocities in granular soils. *J. Soil Mech. Found. Div. ASCE*, 89: SM1:33–65, 1963.
114. Yimin Jiang and Mario Liu. Granular solid hydrodynamics (GSH): a broad-ranged macroscopic theory of granular media. *Acta Mechanica*, 225(8):2363–2384, 2014.
115. L. Bocquet, W. Losert, D. Schalk, T. C. Lubensky, and J. P. Gollub. Granular shear flow dynamics and forces: Experiment and continuum theory. *Phys. Rev. E*, 65(1):011307, Dec 2001.
116. V. Ogarko and S. Luding. Equation of state and jamming density for equivalent bi- and polydisperse, smooth, hard sphere systems. *Journal of Chemical Physics*, 136(12), 2012.
117. Vitaliy Ogarko and Stefan Luding. Prediction of polydisperse hard-sphere mixture behavior using tridisperse systems. *Soft Matter*, 9(40):9530–9534, 2013.
118. V. Magnanimo and S. Luding. A local constitutive model with anisotropy for ratcheting under 2D axial-symmetric isobaric deformation. *Granul. Matter.*, 13(3):225–232, 2011.
119. Ken Kamrin. Nonlinear elasto-plastic model for dense granular flow. *Int. J. of Plasticity*, 26:167–188, 2010.
120. Ken Kamrin and Georg Koval. Nonlocal Constitutive Relation for Steady Granular Flow. *Phys. Rev. Lett.*, 108:178301, 2012.